Patients with sporadic FTLD exhibit similar increases in lysosomal proteins and storage material as patients with FTD due to *GRN* mutations

Skylar E. Davis[1], Anna K. Cook[1], Justin A. Hall[1], Yuliya Voskobiynyk[1], Nancy V. Carullo[2], Nicholas R. Boyle[1], Ahmad R. Hakim[1], Kristian M. Anderson[1], Kierra P. Hobdy[1], Derian A. Pugh[1], Charles F. Murchison[1,3], Laura J. McMeekin[4], Micah Simmons[1,4], Katherine A. Margolies[4], Rita M. Cowell[1,4], Alissa L. Nana[5], Salvatore Spina[5], Lea T. Grinberg[5,6], Bruce L. Miller[5], William W. Seeley[5,6] and Andrew E. Arrant[1,2*]

Abstract

Loss of function progranulin (*GRN*) mutations are a major autosomal dominant cause of frontotemporal dementia (FTD). Patients with FTD due to *GRN* mutations (FTD-*GRN*) develop frontotemporal lobar degeneration with TDP-43 pathology type A (FTLD-TDP type A) and exhibit elevated levels of lysosomal proteins and storage material in frontal cortex, perhaps indicating lysosomal dysfunction as a mechanism of disease. To investigate whether patients with sporadic FTLD exhibit similar signs of lysosomal dysfunction, we compared lysosomal protein levels, transcript levels, and storage material in patients with FTD-*GRN* or sporadic FTLD-TDP type A. We analyzed samples from frontal cortex, a degenerated brain region, and occipital cortex, a relatively spared brain region. In frontal cortex, patients with sporadic FTLD-TDP type A exhibited similar increases in lysosomal protein levels, transcript levels, and storage material as patients with FTD-*GRN*. In occipital cortex of both patient groups, most lysosomal measures did not differ from controls. Frontal cortex from a transgenic mouse model of TDP-opathy had similar increases in cathepsin D and lysosomal storage material, showing that TDP-opathy and neurodegeneration can drive these changes independently of progranulin. To investigate these changes in additional FTLD subtypes, we analyzed frontal cortical samples from patients with sporadic FTLD-TDP type C or Pick's disease, an FTLD-tau subtype. All sporadic FTLD groups had similar increases in cathepsin D activity, lysosomal membrane proteins, and storage material as FTD-*GRN* patients. However, patients with FTLD-TDP type C or Pick's disease did not have similar increases in lysosomal transcripts as patients with FTD-*GRN* or sporadic FTLD-TDP type A. Based on these data, accumulation of lysosomal proteins and storage material may be a common aspect of end-stage FTLD. However, the unique changes in gene expression in patients with FTD-*GRN* or sporadic FTLD-TDP type A may indicate distinct underlying lysosomal changes among FTLD subtypes.

Keywords Frontotemporal dementia, Lysosome, Progranulin, TDP-43

*Correspondence:
Andrew E. Arrant
andrewarrant@uabmc.edu
Full list of author information is available at the end of the article

Davis *et al. Acta Neuropathologica Communications*   (2023) 11:70

Page 2 of 19

Introduction

Loss-of-function mutations in progranulin (*GRN*) are a major autosomal dominant cause of frontotemporal dementia (FTD) [10, 29]. Most of these mutations cause progranulin haploinsufficiency [33, 36, 62, 79], which is thought to cause FTD in *GRN* mutation carriers (FTD-*GRN*). The presence of loss-of-function mutations on both *GRN* alleles, resulting in complete progranulin deficiency, causes the lysosomal storage disorder Neuronal Ceroid Lipofuscinosis (NCL) [2, 44, 82], showing that progranulin is necessary for maintaining lysosomal function.

Progranulin is a secreted pro-protein that is trafficked to lysosomes and cleaved into granulins [43, 106]. Progranulin and some granulins facilitate the activity of several lysosomal enzymes, including the protease cathepsin D (CatD) and enzymes involved in glycosphingolipid metabolism. Progranulin and some granulins interact with CatD and enhance its maturation and stability [13, 17, 18, 84, 104]. Progranulin also facilitates maturation of the glycosphingolipid-metabolizing enzymes β-hexosaminidase A (HexA) [26] and β-glucocerebrosidase (GCase) [8, 46, 85, 105] and regulates lysosomal levels of critical co-factors for glycosphingolipid metabolism, including prosaposin [106, 107] and BMP (bis(monoacylglycero)phosphate) [49, 55].

Brains of patients with FTD-*GRN* exhibit numerous lysosomal abnormalities. Cortical samples from patients with FTD-*GRN* have elevated levels of CatD and other lysosomal proteins [40], elevated levels of extracellular vesicles [4], and accumulation of lysosomal storage material [40, 90]. Cortical samples from patients with FTD-*GRN* also show signs of impaired glycosphingolipid metabolism such as reduced GCase activity [8, 85], low levels of BMP [14, 55], and accumulation of gangliosides [14]. These changes may be a sign of lysosomal dysfunction, which might drive FTD-*GRN* pathogenesis by impairing neuronal autophagy and promoting TDP-43 aggregation [24] or by shifting microglia to a reactive phenotype that destroys synapses and promotes TDP-43 mislocalization in neurons [39, 42, 56, 94, 100].

Lysosomal dysfunction may also be involved in pathogenesis of other genetic FTD subtypes [72, 86, 87]. FTD-causing mutations have been found in several genes involved in the autophagy-lysosomal or endolysosomal pathways, including *VCP* [92], *TBK1* [27, 35, 37, 67], *OPTN* [67], and *CHMP2B* [81]. Similar to patients with *GRN* mutations, brains of FTD patients with *CHMP2B* mutations contain higher levels of lysosomal storage material than controls [28]. *C9ORF72*, in which repeat expansions are the most common genetic cause of FTD and ALS, is also involved in aspects of lysosomal function [3, 42].

Given the evidence that lysosomal dysfunction may contribute to pathogenesis of several genetic FTD subtypes [72, 86, 87], it is possible that lysosomal dysfunction might contribute to pathogenesis of sporadic FTD, which comprises most FTD cases. To address this question, we investigated whether the lysosomal abnormalities of FTD-*GRN* patients [8, 40, 85, 90] are also present in patients with sporadic FTD. We began by comparing samples from patients with FTD-*GRN* or sporadic FTLD-TDP type A (frontotemporal lobar degeneration with TDP-43 pathology type A), the same type of TDP-43 pathology that occurs in patients with FTD-*GRN* [58]. To assess the relationship of these lysosomal abnormalities with TDP-43 pathology and neurodegeneration, we analyzed samples of frontal cortex, a degenerated brain region, and occipital cortex, a mostly spared brain region. We then extended this investigation to include a transgenic mouse model of TDP-opathy [93] and additional subtypes of sporadic FTLD-TDP (FTLD-TDP type C) and FTLD-tau (Pick's disease).

Materials and methods

Patient brain samples

Post-mortem brain samples were provided by the Neurodegenerative Disease Brain Bank at the University of California, San Francisco. Brains were donated with the consent of the patients or their surrogates in accordance with the Declaration of Helsinki and the research was approved by the University of California, San Francisco Committee on Human Research. Tissue blocks were dissected from the orbital part of the inferior frontal gyrus and the inferior occipital cortex of 5 controls, 13 patients with FTD-*GRN*, and 7 patients each with sporadic FTLD-TDP type A, FTLD-TDP type C, or Pick's disease. All patients with FTD-*GRN* carried a pathogenic variant in *GRN* and had FTLD-TDP type A identified at autopsy, except one (Table 1, case 11), who had a primary pathology diagnosis of Lewy body disease, with possible early FTLD-TDP type A pathology. Patients with sporadic FTLD-TDP Type A carried no pathogenic *GRN* variants, though one (Table 1, case 21) carried an intronic *GRN* variant of unknown significance. Patient characteristics are provided in Table 1. Clinical and neuropathological diagnoses were made using standard diagnostic criteria [38, 58, 59, 64, 69].

Animals

Mice expressing wild-type human *TARDBP* under control of the *Thy-1* promoter (TDP++) [93] were obtained from the Jackson Laboratory (#012,836). Mice used for this study were on a mixed genetic background, having been crossed from a C57Bl6J/SJL F1 background onto a C57Bl6/J background for 2–4 generations before

Table 1 Description of patients

#	Group	*GRN* Mutation*	Sex	Age at death	Clinical diagnosis**	Primary neuropath diagnosis***	PMI (h)
1	Ctrl	n/a	F	81	MCI, amnestic	Braak 2	30.3
2	Ctrl	n/a	M	77	MCI, executive	AGD	4.9
3	Ctrl	n/a	F	86	Control	CVD; AGD	7.8
4	Ctrl	n/a	M	76	Control	Braak 2, limbic AGD	8.2
5	Ctrl	n/a	F	86	Control	iLBD, brainstem predominant	6.4
6	GRN	c.1145del:p.Thr382Serfs*30	M	74	nfvPPA/CBS	FTLD-TDP-A	30.9
7#	GRN	c.347C > A:p.Ser116*	M	68	bvFTD	FTLD-TDP-A	13.5
8	GRN	c.264 + 2 T > C	F	73	nfvPPA/CBS	FTLD-TDP-A	20.7
9	GRN	c.1477C > T:p.Arg493*	F	66	bvFTD	FTLD-TDP-A	7.4
10	GRN	c.709-2A > G	M	64	bvFTD	FTLD-TDP-A	7.2
11	GRN	c.1256_1263dup:p.Ile422Glufs*72	M	66	DLB	LBD, FTLD-TDP-A	10.1
12	GRN	c.1A > T:p.Met1?	F	59	CBS	FTLD-TDP-A	9.5
13	GRN	c.1477C > T:p.Arg493*	F	70	PPA, unspecified	FTLD-TDP-A	9.1
14	GRN	c.1216C > T:p.Gln406*	F	56	bvFTD	FTLD-TDP-A	7.6
15	GRN	c.349 + 1G > A	F	78	mixed FTD	FTLD-TDP-A	19
16	GRN	c.328C > T:p.Arg110*	F	66	bvFTD	FTLD-TDP-A	17.1
17	GRN	c.708 + 1G > A	F	64	CBS	FTLD-TDP-A	10.5
18	GRN	c.1256_1263dup:p.Ile422Glufs*72	M	72	AD-type dementia	AD, FTLD-TDP-A	7.2
19	TDP-A	n/a	F	78	nfvPPA	FTLD-TDP-A	9
20	TDP-A	n/a	F	66	CBS	FTLD-TDP-A	17.3
21	TDP-A	n/a†	M	72	PPA-mixed	FTLD-TDP-A	23.8
22	TDP-A	n/a	M	63	CBS	FTLD-TDP-A	15.7
23	TDP-A	n/a	M	70	bvFTD	FTLD-TDP-A	8.5
24	TDP-A	n/a	F	73	bvFTD	FTLD-TDP-A	7.4
25	TDP-A	n/a	F	78	AD-type dementia vs. FTD	FTLD-TDP-A	8.1
26	TDP-C	n/a	F	69	svPPA	FTLD-TDP-C	10.7
27	TDP-C	n/a	M	66	svPPA	FTLD-TDP-C	10
28	TDP-C	n/a	F	68	svPPA	FTLD-TDP-C	8.4
29	TDP-C	n/a	M	66	svPPA	FTLD-TDP-C	14.5
30	TDP-C	n/a	M	75	svPPA	FTLD-TDP-C	3.8
31	TDP-C	n/a	F	75	svPPA	FTLD-TDP-C	7.9
32	TDP-C	n/a	F	71	svPPA	FTLD-TDP-C	13
33	Pick's	n/a	M	64	CBS	Pick's Disease	13.7
34	Pick's	n/a	F	78	nfvPPA	Pick's Disease	14.5
35	Pick's	n/a	F	67	AD-type dementia	Pick's Disease	6.8
36	Pick's	n/a	F	63	nfvPPA	Pick's Disease	4.3
37	Pick's	n/a	M	57	bvFTD	Pick's Disease	12.4
38	Pick's	n/a	F	73	nfvPPA	Pick's Disease	9.6
39	Pick's	n/a	M	78	svPPA	Pick's Disease	7.5

*All *GRN* mutations were heterozygous. **Disease considered most likely to explain the clinical syndrome. ***No control subject had limbic TDP-43 proteinopathy. #case 7 was only analyzed for lysosomal storage markers in fixed tissue. †case 21 was negative for pathogenic *GRN* mutations, but had intronic *GRN* variants of unknown significance. *PMI* postmortem interval, *AD* Alzheimer's disease, *AGD* argyrophilic grain disease, *bvFTD* behavioral variant frontotemporal dementia, *CBS* corticobasal syndrome, *DLB* dementia with Lewy bodies, *LBD* Lewy body disease, *MCI* mild cognitive impairment, *nfvPPA* nonfluent variant primary progressive aphasia, *svPPA* semantic variant primary progressive aphasia

use. Hemizygous transgenic mice were bred to produce nontransgenic and homozygous transgenic littermates for all experiments. Due to the severe motor deficits of homozygous transgenic mice of this line [93], mice were euthanized at 21 days of age for collection of brain samples. Both male and female mice were studied. Mice were housed in a facility accredited by the Association for Assessment and Accreditation of Laboratory Animal Care on a 12 h light/dark cycle with lights on at 6:00 AM. Mice had free access to food (Envigo #7917) and water

Davis *et al. Acta Neuropathologica Communications*   (2023) 11:70

Page 4 of 19

throughout the study. All experiments were approved by the Institutional Animal Care and Use Committee of the University of Alabama at Birmingham.

Tissue preparation

Prior to analysis by enzyme activity assays or immunoblot, tissue from frontal or occipital cortex of patients with FTD or frontal cortex of TDP-43 transgenic mice was homogenized in lysis buffer (50 mM Tris, 150 mM NaCl, 5 mM EDTA, 1% Triton X-100, 0.1% sodium deoxycholate) and centrifuged for 10 min at $5000 \times g$. For analysis of Triton-insoluble p-TDP-43, the resulting pellets were solubilized in 8 M urea. Protein concentration was determined by BCA assay (ThermoFisher) and uniform amounts of protein were used for subsequent activity assays and SDS-PAGE. Two samples were analyzed from each tissue block and averaged to give final results for each patient.

Lysosomal enzyme activity assays

HexA and GCase activity were determined as previously described [8] using fluorogenic substrates (HexA-4-methylumbelliferyl-2-acetamido-2-deoxy-6-sulfate-β-D-glucopyranoside, Research Products International, GCase-4-Methylumbelliferyl β-D-glucopyranoside, MilliporeSigma) conjugated to the fluorophore 4-methylumbelliferone (4-MU). Fluorescence was measured using a Biotek Synergy LX plate reader and quantified relative to a standard curve of 4-MU run on each plate.

CatD activity was determined as previously described [7] using the fluorogenic cathepsin D/E substrate (7-methoxycoumarin-4-yl)acetyl-GKPILF ~ FRLK(2,4-dinitrophenyl)-D-R-NH$_2$ (MilliporeSigma) [97]. Specific CatD activity was determined by subtracting fluorescence generated in the presence of the CatD inhibitor pepstatin A (Fisher Scientific). Lysates were incubated with substrate for 60 min at 37 °C prior to reading fluorescence on a Biotek Synergy LX plate reader. Fluorescence was normalized to control samples run on the same plate.

Immunoblotting

Samples were subjected to SDS-PAGE on 10% TGX polyacrylamide gels (Bio-Rad) prior to transferring to Immobilon-FL PVDF membranes (MilliporeSigma). Membranes were blocked with protein-free blocking buffer (Thermo Scientific) before overnight incubation with primary antibody at 4 °C. The following day, membranes were incubated with species-matched IR-dye–conjugated secondary antibodies (Li-COR Biosciences) and scanned on an Odyssey scanner (Li-COR Biosciences). In some cases, blots were stripped (62.5 mM Tris, pH 6.7, 4% SDS, 85 mM β-mercaptoethanol) and re-probed for additional proteins. Bands were quantified

using ImageStudio Lite software (Li-COR Biosciences), with the exception of low molecular weight GCase, which was quantified using ImageJ to enable clear separation from mature GCase.

Immunostaining

Formalin-fixed blocks of the orbital part of the inferior frontal gyrus or inferior occipital cortex were provided by the Neurodegenerative Disease Brain Bank at the University of California, San Francisco, as described above. Brains from TDP-43 transgenic mice were prepared by transcardial perfusion with 0.9% saline, bisection into hemibrains, and 48-h post-fixation in 4% paraformaldehyde. All tissue was cryoprotected in 30% sucrose and cut into 30 μm sections on a sliding microtome (Leica).

Prior to immunostaining, sections from patient tissue were subjected to antigen retrieval in 10 mM sodium citrate, pH 6.0 at 80°C for 2 h. Mouse brain sections did not require antigen retrieval. The sections were immunostained by overnight incubation with primary antibody, followed by species-matched secondary antibodies, as previously described [66]. Species-matched AlexaFluor-conjugated secondary antibodies (ThermoFisher) were used for immunofluorescence and autofluorescence was quenched using 1% Sudan Black B (Acros Organics). Biotinylated secondary antibodies (Vector Laboratories) and VectaStain Elite ABC reagent (Vector Laboratories) were used for chromogenic labeling with diaminobenzidene (MP Biomedicals).

Antibodies

Antibodies used in this study are described in Table 2.

Autofluorescence

Brain sections from frontal and occipital cortex were washed with PBS, mounted onto Colorfrost Plus slides (Fisher Scientific), and coverslipped with Vectashield HardSet mounting medium containing DAPI (Vector Laboratories). Colocalization of autofluorescence with cell type markers was assessed by immunostaining for MAP2, Iba1, or GFAP as described above, but without quenching autofluorescence with Sudan Black B dye.

Sudan black B staining

Brain sections were mounted onto Colorfrost Plus slides (Fisher Scientific) and dried overnight prior to staining. Slides were then washed twice with water, immersed in 70% ethanol for one minute, then stained for 20 min in 0.1% Sudan Black B (Acros Organics) in 70% ethanol. Slides were then washed twice each with PBS and water before coverslipping with Vectashield HardSet mounting medium (Vector Laboratories).

Davis *et al. Acta Neuropathologica Communications*   (2023) 11:70

Page 5 of 19

Table 2 Antibodies used for Immunoblotting and Immunostaining

Target	Application	Sample Type	Source/Cat. #	Dilution
CatD	IB	Patient	Santa Cruz Biotechnology, sc-	1:500
	IF		6486	1:500
CatD	IB	Mouse	R&D Systems, AF1029	1:500
	IF			1:1000
GCase	IB	Patient	MilliporeSigma, G4171	1:500
GCase	IF	Patient	R&D Systems, MAB7410	1:250
GFAP	IF	Patient/Mouse	Agilent, Z033429	1:1000
HexA	IB	Patient	Santa Cruz Biotechnology, sc-376777	1:500
HexA	IB	Mouse	Abcam, ab189865	1:500
Iba1	IF	Patient/Mouse	Wako, 019–19,741	1:500
LAMP-1	IB	Patient	Santa Cruz Biotechnology, sc-20011	1:1000
LAMP-1	IB	Mouse	Developmental Studies Hybridoma Bank, 1D4B	1:100
LAMP-2	IB	Patient	Santa Cruz Biotechnology, sc-18822	1:1000
MAP2	IF	Patient	ThermoFisher, PA1-10,005	1:1000
NeuN	IF	Patient	Abcam, ab177487	1:1000
NeuN	IF	Mouse	MilliporeSigma, Abn91	1:500
p-TDP-43 (Ser409/410)	IF	Mouse	Proteintech, 22,309–1-AP	1:1000
	IHC			1:60,000
	IB	Patient		1:500
SCMAS	IHC	Mouse	Abcam, ab181243	1:500

CatD cathepsin D, *GCase* β-glucocerebrosidase, *HexA* β-hexosaminidase A, *IB* immunoblot, *IF* immunofluorescence, *IHC* immunohistochemistry, *SCMAS* subunit C of mitochondrial ATP synthase

Imaging and analysis

Patient brain sections processed for autofluorescence and Sudan Black B were imaged at 20× on a Nikon upright microscope or an EVOS M5000 imaging system (ThermoFisher). Images were taken of cortical layer II/III from 2–3 sections from each patient and averaged to give final values. The number of autofluorescent or Sudan Black B-positive particles per field of view was determined using ImageJ. Due to variability in background fluorescence and staining, the Triangle autothreshold function [99] was used to detect autofluorescence and the Yen autothreshold function [98] was used to detect Sudan Black B. Preliminary trials with these functions produced very similar thresholds as investigators blinded to sample identity.

Images of p-TDP-43, autofluorescence, and SCMAS from mouse brain sections were taken at 20X on an EVOS M5000 imaging system (ThermoFisher). Staining was quantified with ImageJ by applying a uniform threshold to all images. Immunofluorescent images for colocalization were obtained at 20X on a Nikon Ti2-C2 confocal microscope.

Nanostring analysis

A custom Nanostring nCounter panel was designed to assess expression of 42 endolysosomal genes, with normalization to the housekeeping genes *AARS*, *CCDC12*, *FAM104A*, *HPRT1*, and *PGK1*. RNA was extracted from samples of frontal and occipital cortex using the Qiagen RNEasy kit, then 200 ng of RNA from each sample was analyzed using an nCounter analysis system (Nanostring) and nSolver 4.0 software (Nanostring) in UAB's Nanostring laboratory.

qPCR

For mouse brain samples, quantitative reverse-transcription PCR was performed as previously described [34]. RNA was extracted from frontal cortex of nontransgenic and TDP++ littermates with Trizol (ThermoFisher). RNA samples were treated with DNase (Promega), then reverse transcribed with the High Capacity cDNA Reverse Transcription Kit (ThermoFisher). qPCR was conducted using Taqman assays (ThermoFisher) for *Hexa* (Mm00599877_m1), *Ctsd* (Mm00515586_m1), *Gusb* (Mm01197698_m1), *Atp6v1a* (Mm01343719_m1), *Atp6v0a2* (Mm00441838_m1), *Lamp1* (Mm00495262_m1), *Cd63* (Mm01966817_g1), *Cd9* (Mm00514275_g1), and *Grn* (Mm01245914_g1) using JumpStart Taq Readymix (MilliporeSigma), and normalized to expression of *Actb* (Mm00607939_s1).

For patient samples, RNA was extracted with the Qiagen RNEasy kit, treated with DNase (ThermoFisher),

and reverse transcribed using Biorad iScript. qPCR was conducted using pre-designed Prime-Time qPCR primers (Integrated DNA Technologies) and Power SYBR Green master mix (ThermoFisher). The following primer sets were used: *HEXA* (Hs.PT.58.24457208), *CTSD* (Hs.PT.58.27568031), *GUSB* (Hs.PT.58v.27737538), *IDUA* (Hs.PT.58.40058589), *LAMP1* (Hs.PT.58.27192505), *CD63* (Hs.PT.58.25219306), *GRN* (Hs.PT.58.2528960.g), and *PSAP* (Hs.PT.58.744083), and normalized to expression of *HPRT1* (Hs.PT.58v.45621572). Two samples were analyzed from each tissue block and averaged to give final results for each patient.

Small molecule fluorescent in situ hybridization (FISH)

Small molecule fluorescent in situ hybridization (FISH, RNAscope) was performed to localize and quantify transcript for *Ctsd* (cat #520,571, Advanced Diagnostics/ACD) in mouse brain tissue. Brains from non-transgenic or TDP++ mice were fresh frozen on dry ice, sectioned at 20 μm on a cryostat, and re-frozen at -80° C until use. FISH was performed according to manufacturer's instructions and as previously described [34], using four mice/group, four coronal hemisections/mouse. Cortical glutamatergic neurons and parvalbumin-expressing interneurons were identified using probes for *Slc17a7* (cat #416,631-C2, Advanced Diagnostics) and *Pvalb* (cat #421,931-C3, Advanced Diagnostics), respectively, using the RNAscope Mulitplex Fluorescent Assay V1 (Advanced Diagnostics). Images were collected on a Nikon A1+confocal microscope and exported as tiffs into ImageJ for analysis [34, 76, 80]. Thresholds were set using samples from non-transgenic mice, regions of interest were selected by *Slc17a7* or *Pvalb*-positivity in the same sections, and *Ctsd* was quantified by region-of-interest, taking into consideration the area of the cell (generating a mean pixel density value).

Electron microscopy

Frontal cortices were rapidly dissected after euthanizing mice, then fixed overnight at 4 °C in 6% glutaraldehyde and 2% paraformaldehyde in 0.15 M cacodylate buffer with 1 mM Ca^{++} and 2 mM Mg^{++}. The following day, the tissue was rinsed three times in 0.15 M cacodylate buffer, then post-fixed for 90 min at room temperature in 1% osmium tetroxide in 0.15 M cacodylate buffer. The tissue was then rinsed three more times and processed through a graded ethanol series followed by three changes in propylene oxide. The tissue was infiltrated overnight with a 1:1 solution of propylene oxide and Epon-812 resin, followed by three incubations in 100% resin for two hours each. Tissue pieces were arranged in embedding molds, embedded in fresh resin, and polymerized at 65 °C overnight. The samples were then sliced, mounted onto copper grids, and imaged on a Technai Spirit T12 transmission electron microscope (ThermoFisher).

Statistics

Most data are shown in box and whisker plots with the box drawn from the 25th to 75th percentiles, a line at the median value, and whiskers extending to the minimum and maximum data points. Tables containing all patient data are available in Additional File 2. For all analyses, two-tailed *p* values were calculated with α set at 0.05. Data were tested for unequal variance using Bartlett's test or F test, and for non-normal distribution using the D'Agostino-Pearson test in GraphPad Prism 9. Data that failed to meet assumptions of equal variance or normality were either log-transformed or analyzed by nonparametric tests. Except where noted, data were analyzed with GraphPad Prism 9.

Enzyme activity, protein levels, Triton-insoluble p-TDP-43, and lysosomal storage material in patient samples were analyzed by one-way ANOVA with a factor of patient group. Significant group effects were followed by Fisher's LSD post-hoc test. Due to unequal variance, levels of low molecular weight GCase, Triton-insoluble p-TDP-43, and lysosomal storage material in patients were log-transformed prior to analysis. The relationship between p-TDP-43 and lysosomal protein levels was assessed using Spearman correlation. Mouse enzyme activity and protein levels were analyzed by *t* test, and *Ctsd* in situ hybridization was analyzed with Mann–Whitney test (mean values per mouse) or Kolmogorov–Smirnov test (cumulative frequency of *Ctsd* labeling). Lysosomal storage material in mice was analyzed with Mann–Whitney test. Due to analysis of multiple genes that were expected to exhibit similar changes relative to controls, qPCR data from both patient and mouse samples were analyzed by MANOVA using IBM SPSS Statistics 27. Group significance for individual genes was determined by between-subjects test. For patient qPCR data, this was followed with pair-wise comparisons between patient groups using Tukey's post-hoc test. Due to unequal variance, both patient and mouse qPCR data were log-transformed prior to analysis.

Analyses of Nanostring data were conducted with R 4.0 with additional utility from the Bioconductor suite of packages, with specific application of the Limma, Glimma, and DeSeq2 packages. Nanostring data were analyzed with general linear mixed-effects models to evaluate the impact of patient group on differential expression of mRNA. Abundance of mRNA profiles assumed a Gamma distribution using a natural log link function to account for the right-skewed scale distribution. Once samples were normalized to adjust for batch effects, GLME models were applied to each of transcripts

Davis *et al. Acta Neuropathologica Communications*   (2023) 11:70

Page 7 of 19

of interest with fixed effects covariates for brain region (occipital vs orbital), patient group (control vs FTD-*GRN* vs sporadic FTLD-TDP type A) and their interaction. Random effects blocked on individual patients who provided tissue from both brain regions. Specific contrasts of interest identified group effects between control patients and the two groups of patients with FTLD while controlling for brain region effects. For significance of differential expression between patients with FTD-*GRN* or sporadic FTLD-TDP type A versus controls, changes in mRNA expression for patients required a minimum 50% fold change in either direction relative to controls to be considered clinically meaningful, with statistical significance for *p*-values less than 0.05 after False Discovery Rate correction of 5% to account for multiple comparisons.

Results

Similar increases in lysosomal proteins in frontal cortex of patients with FTD-GRN and sporadic FTLD-TDP type A

Prior reports show that frontal cortex from patients with FTD-*GRN* has elevated levels of CatD, HexA, and other lysosomal proteins [8, 40], as well as reduced levels of mature GCase and accumulation of incompletely glycosylated GCase [8, 85]. We therefore analyzed frontal cortex from controls, patients with FTD-*GRN*, and patients with sporadic FTLD-TDP type A for CatD, HexA, and GCase enzyme activity and protein levels.

Across all measures, patients with FTD-*GRN* and sporadic FTLD-TDP type A exhibited similar changes relative to controls. Both patient groups exhibited elevated HexA activity (Fig. 1a), as well as elevated levels of mature CatD and the lysosomal membrane proteins LAMP-1 and LAMP-2 (Fig. 1b). In contrast to prior observations [8, 85], neither group exhibited a deficit in GCase activity (Fig. 1a) or mature GCase protein levels
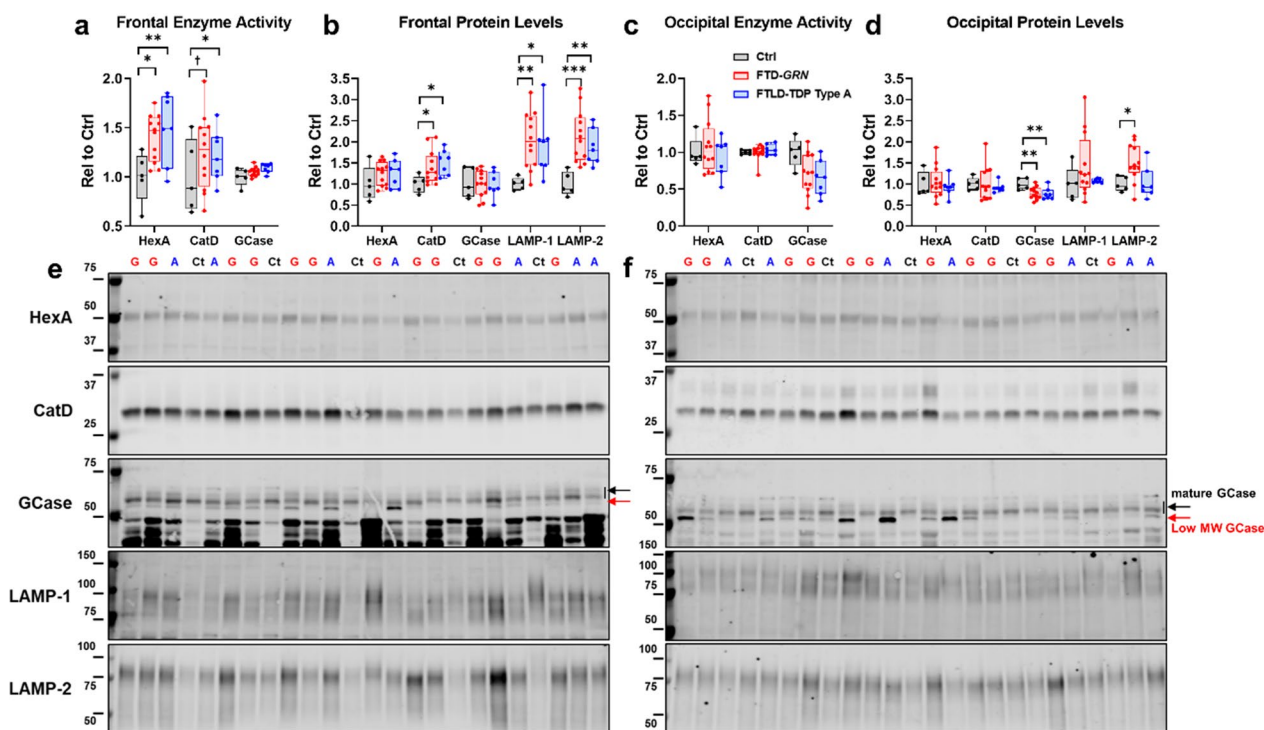

Fig. 1 Increases in lysosomal enzyme activity and protein levels in frontal cortex of patients with FTD-*GRN* and sporadic FTLD-TDP type A. **a** Analysis of lysates from frontal cortex of patients with FTD-*GRN* or sporadic FTLD-TDP type A revealed similar increases in HexA activity (ANOVA, *p* = 0.0171) and CatD activity (ANOVA, *p* = 0.0404) in each patient group. No changes in GCase activity were detected (ANOVA, *p* = 0.4053). **b** Lysosomal protein levels followed a similar pattern, with both patient groups exhibiting increased levels of mature CatD (ANOVA, *p* = 0.0429), LAMP-1 (ANOVA, *p* = 0.0170), and LAMP-2 (ANOVA, *p* = 0.0019). **c** In contrast, no significant changes in enzyme activity were detected in occipital cortex, though there was a trend for reduced GCase activity in FTD patients (ANOVA, *p* = 0.0595). **d** Levels of mature GCase protein were reduced in occipital cortex of both patient groups (ANOVA, *p* = 0.0159) and the only elevated lysosomal protein in occipital cortex was LAMP-2, which was only elevated in patients with FTD-*GRN* (ANOVA, *p* = 0.0232). Immunoblots for frontal cortex are shown in **e** and for occipital cortex are shown in **f**. HexA = β-hexosaminidase A, CatD = cathepsin D, GCase = β-glucocerebrosidase. In **e**, **f** Ct = control, G = FTD-*GRN*, and A = sporadic FTLD-TDP type A. Molecular weight markers are identified by weight in kDa for each blot. †*p* < 0.1, **p* < 0.05, **p < 0.01, and ***p < 0.001 by Fisher's LSD post-hoc test. n = 5 controls, 12 patients with FTD-*GRN*, and 7 patients with sporadic FTLD-TDP type A

(Fig. 1b). Most patients from both FTLD groups exhibited a low molecular weight GCase band that we previously found to be composed of incompletely glycosylated GCase (Fig. 1e) [8]. This band was very faint in all but one control. Levels of this low molecular weight GCase were significantly elevated versus controls in patients with sporadic FTLD-TDP type A (Additional file 1: Fig. S1), with a similar trend in patients with FTD-*GRN.*

Limited changes in lysosomal proteins in occipital cortex of patients with FTD-GRN and sporadic FTLD-TDP type A

To determine whether these lysosomal changes were limited to a degenerated brain region, we measured the same lysosomal markers in occipital cortex, a region that was relatively spared from FTLD-TDP pathology.

In occipital cortex, neither patient group exhibited changes in HexA or CatD (Fig. 1c,d), but there was a trend for reduced GCase activity (Fig. 1c, ANOVA $p = 0.0595$) in both FTLD patient groups. Levels of mature GCase were significantly reduced in both FTLD patient groups (Fig. 1d), many of whom exhibited some accumulation of low molecular weight GCase (Fig. 1e), though levels of low molecular weight GCase did not statistically differ from controls (Additional file 1: Fig. S1). LAMP-1 levels were not significantly elevated in either FTLD patient group, but LAMP-2 levels were elevated in patients with FTD-*GRN* (Fig. 1d). In summary, the increases in lysosomal activity and protein levels were largely limited to frontal cortex in both FTLD patient groups.

Association of increased CatD and LAMP-1 with accumulation of p-TDP-43 in frontal cortex

The more dramatic increase in lysosomal proteins in frontal cortex than in occipital cortex of patients with FTD-*GRN*, as well as the presence of similar increases in patients with sporadic FTLD-TDP type A, suggested that these changes may be more associated with aspects of FTLD-TDP type A pathology such as TDP-opathy, neurodegeneration, or neuroinflammation than with progranulin insufficiency. To gain insight into the relationship of TDP-opathy with increases in lysosomal proteins, we conducted immunoblots for p-TDP-43 (Ser409/410) on the Triton-insoluble pellets from lysates used to determine enzyme activity and protein levels. These immunoblots revealed a roughly 25 kDa p-TDP-43 band that was detectable only in patients with FTD-*GRN* or sporadic FTLD-TDP type A (Additional file 1: Fig. S2a,b). Both patient groups exhibited similar levels of 25 kDa p-TDP-43 on average, so we analyzed the correlation across FTLD groups of 25 kDa p-TDP-43 with levels of proteins that were significantly elevated in patients with

FTLD: CatD, LAMP-1, LAMP-2, and low molecular weight GCase (Additional file 1: Fig. S2c–f). These analyses revealed a significant correlation of 25 kDa p-TDP-43 with CatD and LAMP-1, with a similar trend for LAMP-2. Levels of low molecular weight GCase were not correlated with levels of 25 kDa p-TDP-43.

Cellular distribution of altered lysosomal proteins in frontal cortex of patients with FTD-GRN and sporadic FTLD-TDP type A

Since neuroinflammation could be an important factor driving the increase in lysosomal proteins in the frontal cortex, we conducted co-immunotaining to investigate whether these proteins were highly expressed in glia. We immunostained for progranulin, CatD, and GCase with markers of neurons (NeuN), microglia (Iba1), and astrocytes (GFAP) in frontal cortex of controls and patients with FTD-*GRN* or sporadic FTLD-TDP type A. Consistent with a prior report [25], we observed strong progranulin immunoreactivity in microglia (Additional file 1: Fig. S3a), suggesting that high progranulin expression by reactive microglia may mask the progranulin haploinsufficiency of patients with *GRN* mutations.

In contrast, we observed robust CatD immunoreactivity in neurons from both patient groups (Additional file 1: Fig. S3b), as well as some labeling in both microglia and astrocytes. Based on this labeling pattern, the increased CatD activity in FTLD patient tissue could be driven by changes in both neurons and glia.

Consistent with our prior observations [8], we observed lower GCase immunoreactivity in neurons from frontal cortex of patients with FTD-*GRN* (Additional file 1: Fig. S3c), but also observed some GCase immunoreactivity in astrocytes. Astrogliosis might therefore explain why we did not observe lower mature GCase levels in lysates of frontal cortex of patients with FTD-*GRN*, but did observe lower GCase levels in occipital cortex, which should have less neuroinflammation in these patients.

Similar increases in lysosomal transcript levels in frontal cortex of patients with FTD-GRN and sporadic FTLD-TDP type A

Having seen similar region-dependent changes in a small set of lysosomal proteins among patients with FTD-*GRN* and sporadic FTLD-TDP type A, we analyzed the expression of 42 lysosomal genes using a Nanostring panel to gain a broader view of lysosomal changes in these patients. This panel consisted of transcripts for late endosomal and lysosomal membrane proteins, enzymes, and ion channels (Fig. 2a). In frontal cortex, the majority of genes on the panel trended toward increased expression relative to controls (Fig. 2a), with a total of 21 genes
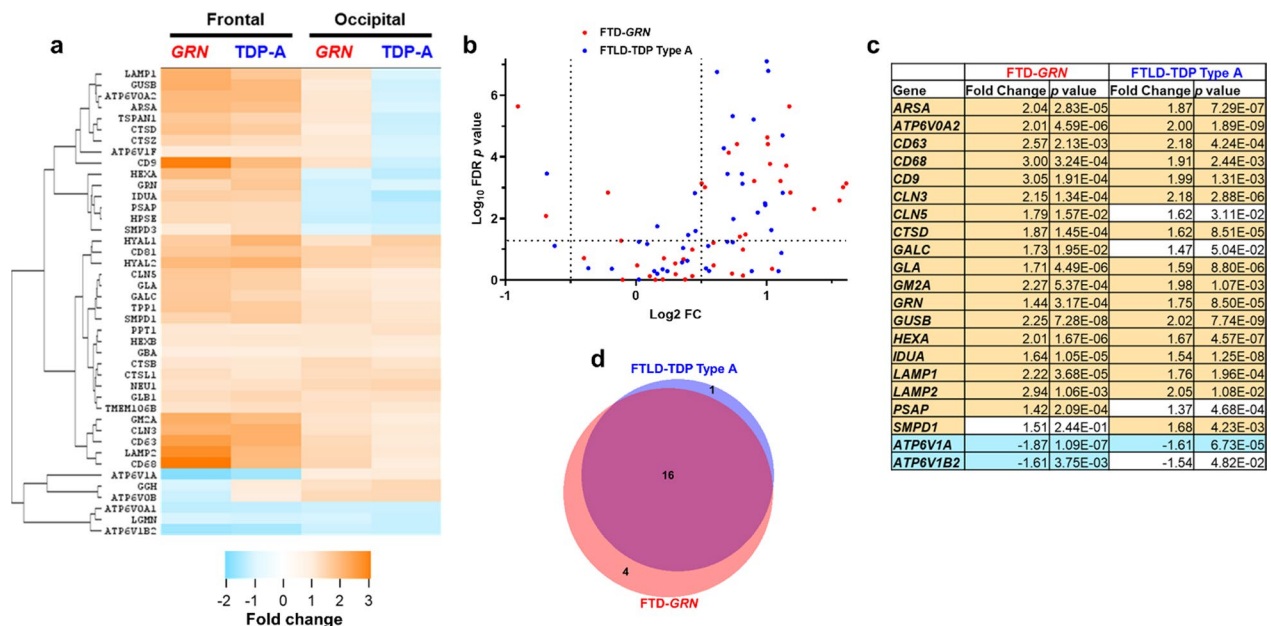
Davis *et al. Acta Neuropathologica Communications* (2023) 11:70

Page 9 of 19

Fig. 2 Similar changes in lysosomal gene expression in patients with FTD-*GRN* and sporadic FTLD-TDP type A. **a** Nanostring analysis of 42 genes related to endolysosomal function revealed similar changes in gene expression in frontal cortex of patients with FTD-*GRN* and patients with sporadic FTLD-TDP type A. **b**, **c** Statistical analysis revealed 20 differentially expressed genes versus control in frontal cortex across both patient groups, with no significant changes versus control in occipital cortex. **c**, **d** There was strong overlap of differentially expressed genes across both patient groups, with 16/20 genes exhibiting altered expression in both groups. Shaded cells in **c** indicate statistical significance after correction for multiple comparisons. n = 5 controls, 12 patients with FTD-*GRN*, and 7 patients with sporadic FTLD-TDP type A. In **a** GRN = FTD-*GRN* and TDP-A = FTLD-TDP type A

reaching statistical significance (Fig. 2b,c). Of these 21 genes, 16 were shared between patients with FTD-*GRN* and sporadic FTLD-TDP type A (Fig. 2d). Consistent with enzyme activity and immunoblots, transcripts for *HEXA*, *CTSD*, *LAMP1*, and *LAMP2* were more abundant in each patient group relative to controls (Fig. 2c). *GRN* was also elevated in both patient groups, consistent with a prior study of patients with FTD-*GRN* [25]. Two genes encoding vacuolar ATPase subunits were downregulated, one of which was shared between patients with FTD-*GRN* and FTLD-TDP type A (Fig. 2b,c). In occipital cortex, no changes in gene expression reached statistical significance (Fig. 2a).

Patients with FTD-GRN and sporadic FTLD-TDP type A exhibit signs of lysosomal storage material in frontal cortex

We next analyzed accumulation of lysosomal storage material by measuring autofluorescence and staining with Sudan Black B. Consistent with a prior report [90], patients with FTD-*GRN* had more autofluorescent (Fig. 3a,b) and Sudan Black B-positive particles (Fig. 3d,e) in frontal cortex than controls. Patients with sporadic FTLD-TDP-A had more Sudan Black B-positive particles in frontal cortex than controls (Fig. 3d,e), but did

not have more autofluorescent particles. Neither FTLD patient group had significantly elevated autofluorescence (Fig. 3c) or Sudan Black B labeling (Fig. 3f) in occipital cortex, though patients with FTD-*GRN* had a trend for increased levels of Sudan Black B-positive particles (ANOVA, *p* = 0.0819).

A mouse model of TDP-opathy replicates the increased CatD expression and accumulation of lysosomal storage material observed in FTLD-TDP type A patients

Since patients with FTD-*GRN* and sporadic FTLD-TDP type A had similar lysosomal abnormalities that were generally limited to the degenerated frontal cortex and some of which were associated with levels of p-TDP-43 (Additional file 1: Fig. S2), we hypothesized that TDP-opathy, neurodegeneration, and/or neuroinflammation might be sufficient to drive these lysosomal abnormalities. To test this hypothesis, we analyzed lysosomal phenotypes in a transgenic mouse model of TDP-opathy that expresses wild-type human TDP-43 under control of the *Thy1* promoter [93]. When bred to homozygosity (TDP++ mice), these mice exhibit TDP-43 aggregation (Additional file 1: Fig. S4), neuronal loss, and gliosis [93] by 21 days of age.
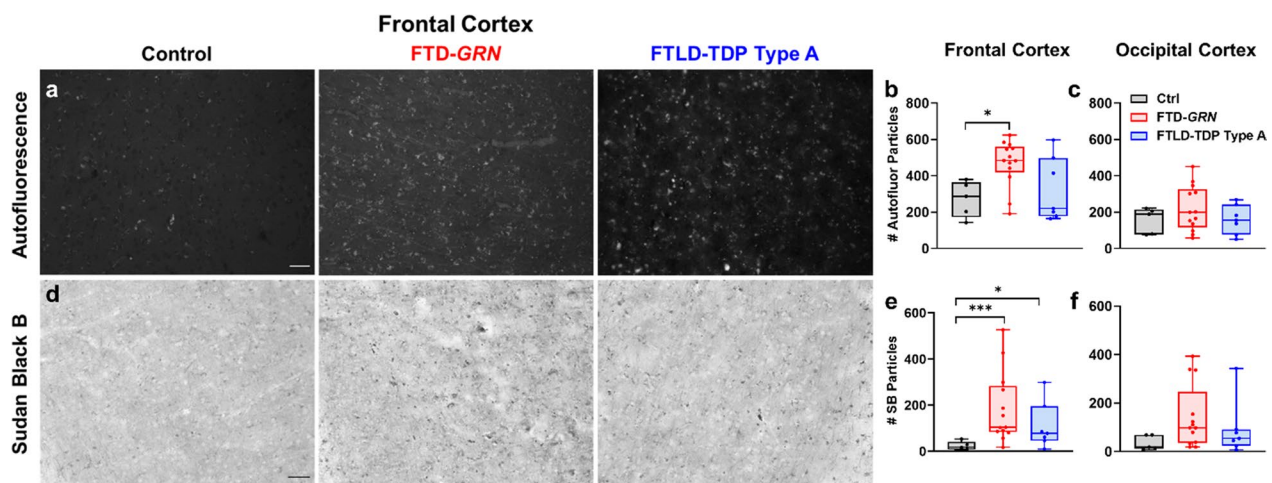
Fig. 3 Signs of lysosomal storage material in frontal cortex of patients with FTD-*GRN* or sporadic FTLD-TDP type A. Patients with FTD-*GRN* exhibited a greater number of autofluorescent particles than controls in frontal cortex (ANOVA effect of group, $p = 0.0243$), while patients with sporadic FTLD-TDP type A did not differ from controls. **c** No difference was detected in autofluorescent particles in the occipital cortex of either group versus control (ANOVA effect of group, $p = 0.4988$). **d**, **e** Patients with FTD-*GRN* also exhibited a greater number of Sudan Black B-positive particles than controls in frontal cortex (ANOVA effect of group, $p = 0.0022$), as did patients with sporadic FTLD-TDP type A. **f** Levels of Sudan Black B-positive particles in occipital cortex of patients with FTD-*GRN* or FTLD-TDP type A did not significantly differ from controls (ANOVA effect of group, $p = 0.0819$). Scale bars in **a**, **d** represent 50 μm. *$p < 0.05$ and ***$p < 0.001$ by Fisher's LSD post-hoc test. n = 5 controls, 13 patients with FTD-*GRN*, and 7 patients with sporadic FTLD-TDP type A

Analysis of frontal cortex from 21 day-old TDP++ mice revealed increases in CatD activity and mature CatD levels similar to those observed in FTLD patients (Fig. 4a,b), though HexA and LAMP-1 levels were not significantly altered. Analysis of a subset of genes with differential expression in FTLD patients (Fig. 2) revealed that TDP++ mice replicated the increases in *Ctsd*, *Gusb*, *Lamp1*, and *Cd63* (Fig. 4c), though the mice exhibited an opposite change in *Atp6v0a2* from that observed in patients. As in FTD patients, CatD protein exhibited a heavily neuronal localization (Fig. 4d), and in situ hybridization revealed an increase in *Ctsd* mRNA expression in excitatory (*Slc17a7*+) neurons with no change in expression in local fast-spiking (*Pvalb*+) interneurons (Fig. 4e–g).

We next examined frontal cortex of 21 day-old TDP++ mice for lysosomal storage material by assessing levels of autofluorescence and subunit C of mitochondrial ATP synthase (SCMAS). SCMAS is a marker of lipofuscin [30, 41, 50] that is also elevated in $Grn^{-/-}$ mice [7, 40], which model the lipofuscinosis of homozygous *GRN* carriers [2, 44, 82]. TDP++ mice had higher levels of both autofluorescence (Fig. 4h,i) and SCMAS (Fig. 4j,k) in frontal cortex than nontransgenic littermates, indicating accumulation of lysosomal storage material. Notably, the autofluorescent material was less abundant than observed in patients, perhaps due to the young age of these mice. The autofluorescent material was present in both neurons and microglia, and exhibited a punctate

appearance rather than the granular morphology typical of lipofuscin (Additional file 1: Fig. S5). However, electron microscopy revealed deposits with similar appearance as storage material from $Grn^{-/-}$ mice (Additional file 1: Fig. S5).

In summary, TDP++ mice partially replicated the lysosomal changes of patients with FTD-*GRN* or sporadic FTLD-TDP type A, particularly the increases in *Ctsd* transcript, CatD protein/activity, and potential lysosomal storage material. With the caveat that these data were obtained from young mice that overexpress TDP-43, these findings suggest that TDP-opathy, neurodegeneration, and/or neuroinflammation can drive these changes independently of progranulin haploinsufficiency.

Patients with multiple sporadic FTLD subtypes exhibit similar lysosomal abnormalities as patients with FTD-GRN

To determine whether the lysosomal changes observed in patients with FTD-*GRN* or sporadic FTLD-TDP type A are specifically associated with TDP-opathy or may be more generally associated with neurodegeneration or neuroinflammation, we extended our investigation to include patients with a subtype of FTLD-TDP not associated with *GRN* mutations (type C) or a subtype of FTLD-tau (Pick's disease). For this analysis, new slices were collected from the previously used tissue blocks of frontal cortex from controls and patients with FTD-*GRN* or sporadic FTLD-TDP type A and analyzed in parallel with
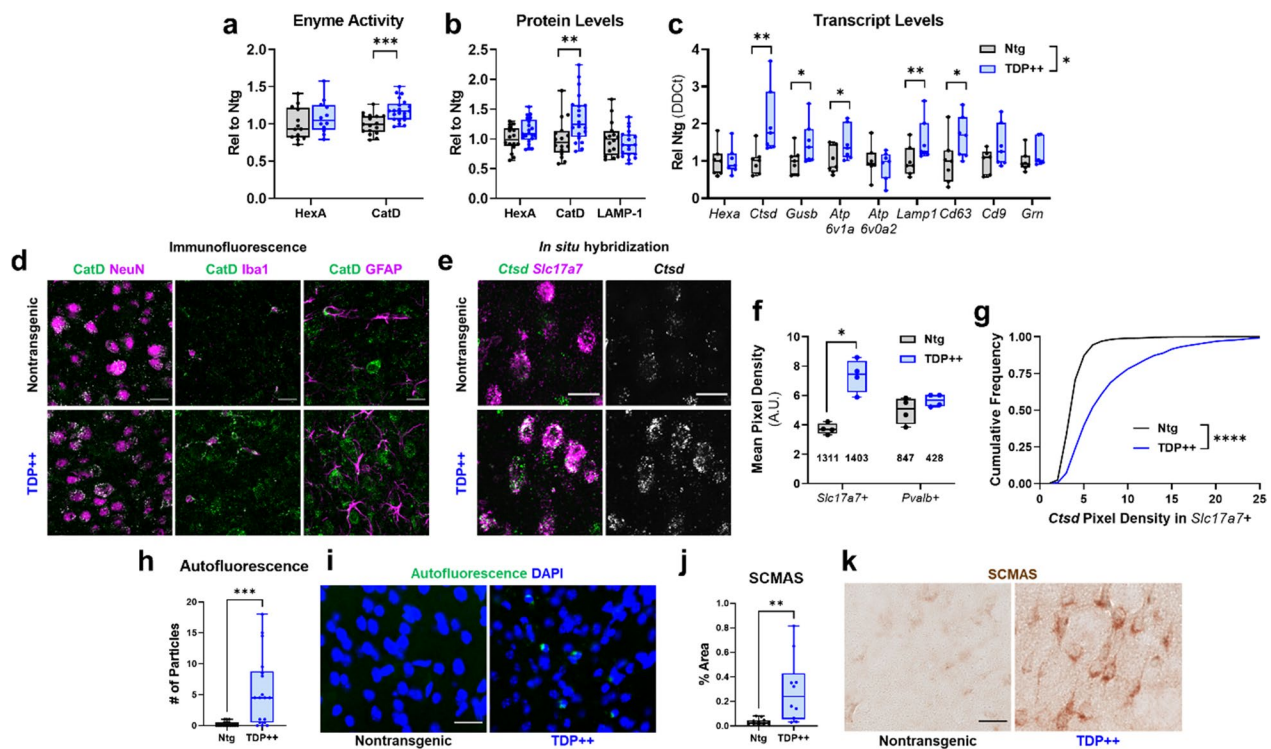
Fig. 4 A mouse model of TDP-opathy partially replicates the lysosomal abnormalities observed in patients with FTD-*GRN* or sporadic FTLD-TDP type A. **a** Homozygous TDP-43 transgenic mice (TDP++) had elevated CatD activity versus nontransgenic littermates (*t* test, $p = 0.0004$, $n = 17$–21 mice per genotype), though HexA activity did not differ between groups. **b** TDP++ mice had a corresponding increase in mature CatD levels (*t* test, $p = 0.0075$, $n = 16$–21 mice per genotype), but no significant changes in HexA (*t* test, $p = 0.0704$) or LAMP-1 (*t* test, $p = 0.3807$). **c** TDP++ mice also exhibited increases in several lysosomal genes that were elevated in patients with FTLD (MANOVA effect of genotype, $p = 0.019$, $n = 7$ mice per genotype). **d** CatD immunoreactivity in TDP++ mice was mostly neuronal, but also present in glia. **e**–**g**, in situ hybridization for *Ctsd* confirmed an increase in *Ctsd* expression in cortical vGlut1-positive (*Slc17a7*+) excitatory neurons (Mann–Whitney test, $p = 0.0286$), but not in parvalbumin-positive interneurons (Mann–Whitney test, $p = 0.3429$, $n = 4$ mice per genotype, number of cells analyzed is noted in **f**). The cumulative frequency of *Ctsd* labeling in *Slc17a7* + excitatory neurons is shown in **g** (Kolmogorov–Smirnov test, $p < 0.0001$). TDP++ mice also accumulated storage material in frontal cortex, with an increase in autofluorescent particles (**h, i** Mann–Whitney test, $p = 0.0002$, $n = 16$–18 mice per genotype) and SCMAS (**j, k** Mann–Whitney, $p = 0.0015$, $n = 10$–11 mice per genotype). Scale bars represent 20 μm in (**d, e, i, k**). *$p < 0.05$, **$p < 0.01$, and ***$p < 0.001$ by *t* test in **a** and **b**, MANOVA between-subjects test in (**c**), ANOVA with Fisher's LSD post-hoc test in (**f**), Kolmogorov–Smirnov test in (**g**), and Mann–Whitney test in (**h, j**)

slices from tissue blocks of frontal cortex from patients with FTLD-TDP type C or Pick's disease.

Analysis of lysosomal enzyme activity revealed a non-significant trend for increased HexA activity (Fig. 5a, ANOVA effect of patient group, $p = 0.1079$) among all FTLD patient groups. CatD activity was significantly increased in patients with FTD-*GRN*, FTLD-TDP type C, and Pick's disease. Similarly, all FTLD patient groups

(See figure on next page.)

Fig. 5 Similar lysosomal protein changes and storage material accumulation in frontal cortex of patients with multiple FTLD subtypes. Frontal cortex from patients with FTD-*GRN*, FTLD-TDP type C, or Pick's Disease exhibited increased CatD activity versus controls (**a**, ANOVA effect of group, $p = 0.0109$). HexA activity was not significantly different from controls (ANOVA effect of group, $p = 0.1079$), though all FTLD groups exhibited trends for increased activity. **b, c** All FTLD patient groups also exhibited at least trends for elevated levels of LAMP-1 (ANOVA effect of group, $p = 0.013$) and LAMP-2 (ANOVA effect of group, $p = 0.0059$). **d, e** Patients with FTD-*GRN* and Pick's disease exhibited higher numbers of autofluorescent particles compared to controls, and patients with FTLD-TDP type A exhibited a similar trend (ANOVA effect of group, $p = 0.0254$). **f, g** All FTLD patient groups had higher numbers of Sudan Black B-positive particles than controls (ANOVA effect of group, $p < 0.0001$). In **a** HexA data are scaled to the left y-axis and CatD data are scaled to the right y-axis. †$p < 0.1$, *$p < 0.05$, **$p < 0.01$, ***$p < 0.001$, and ****$p < 0.0001$ by Fisher's LSD post-hoc test. Black lines and symbols indicate difference from controls. The red line and symbol in **b** indicate difference from FTD-*GRN*. $n = 5$ controls, 12–13 patients with FTD-*GRN*, 7 patients with FTLD-TDP type A, 7 patients with FTLD-TDP type C, and 7 patients with Pick's disease. Abbreviations for **c** are: Ct = control, G = FTD-*GRN*, A = FTLD-TDP type A, C = FTLD-TDP type C, P = Pick's disease. Scale bars in **f** and **g** represent 50 μm
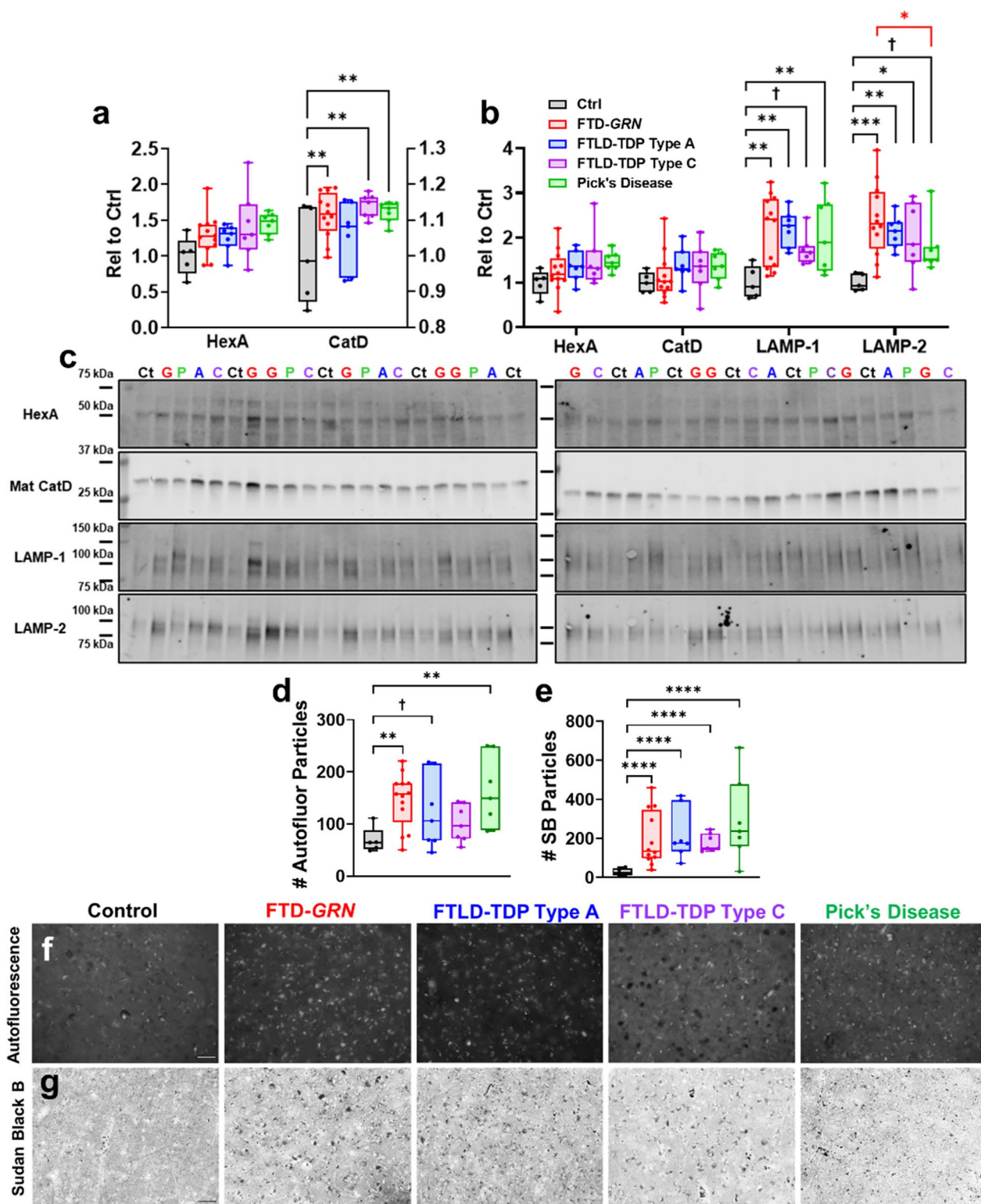
Fig. 5 (See legend on previous page.)

exhibited increases in LAMP-1 and/or LAMP-2 (Fig. 5b) relative to controls. We did not observe significant increases in HexA activity or CatD protein levels versus controls as in Fig. 1, perhaps due to loss of statistical power with the increased number of comparisons.

As in Fig. 1, levels of mature GCase did not differ between controls and patients with FTLD, but patients with FTD-*GRN* or FTLD-TDP type A exhibited significant increases in low molecular weight GCase (Additional file 1: Fig. S6). Patients with FTLD-TDP type C did not accumulate low molecular weight GCase, and had significantly lower levels than patients with FTD-*GRN*. However, patients with Pick's disease had intermediate levels of low molecular weight GCase that did not statistically differ from either controls or patients with FTD-*GRN*.

Analysis of lysosomal storage material revealed an increased number of autofluorescent particles (Fig. 5d,e) in patients with FTD-*GRN* and Pick's disease, with a similar trend for patients with FTLD-TDP type A. All FTLD patient groups exhibited an increase in Sudan Black B-positive particles relative to controls (Fig. 5f,g). Fluorescent immunostaining revealed that neurons and astrocytes accumulated autofluorescent storage material, with microglia exhibiting some storage material as well (Additional file 1: Fig. S7).

In summary, all groups of patients with sporadic FTLD exhibited generally similar changes in lysosomal proteins as patients with FTD-*GRN*. The only exceptions to this trend were lower levels of LAMP-2 in patients with Pick's disease than patients with FTD-*GRN* (Fig. 5b), which still trended higher than controls), and the lack of

accumulation of low molecular weight GCase in patients with FTLD-TDP type C.

Patients with sporadic FTLD-TDP type C or Pick's disease do not exhibit the increased lysosomal transcript levels observed in patients with FTD-GRN or FTLD-TDP type A

In contrast to the generally similar changes in lysosomal proteins, qPCR for a subset of the differentially expressed genes found by Nanostring (Fig. 2) revealed distinct changes in patients with FTD-*GRN* and sporadic FTLD-TDP type A versus the other FTLD subtypes (Fig. 6). qPCR validated the increases in *PSAP*, *HEXA*, *GUSB*, *CD63*, and *LAMP1* for patients with FTD-*GRN* and sporadic FTLD-TDP type A, and in *GRN* for patients with sporadic FTLD-TDP type A (Tukey's post-hoc test for *GRN* in Ctrl vs. *GRN*, $p = 0.078$). *CTSD* and *IDUA* exhibited statistically non-significant trends for increases versus controls (Tukey's post-hoc test, *CTSD* Ctrl vs. *GRN*, $p = 0.056$, *CTSD* Ctrl vs FTLD-TDP-A, $p = 0.089$, *IDUA* Ctrl vs. *GRN*, $p = 0.073$, *IDUA* Ctrl vs. FTLD-TDP-A, $p = 0.065$). In contrast, patients with FTLD-TDP type C or Pick's disease exhibited no significant changes in any of these genes versus controls. Direct comparison between patients with FTD-*GRN* and other FTLD groups revealed that patients with FTD-*GRN* had higher expression of most of these genes than patients with Pick's disease (Fig. 6, red symbols). Thus, while signs of general lysosomal dysfunction were similar across FTLD subtypes (increases in CatD, LAMP1 and LAMP2, and lysosomal storage material), changes in expression of this subset of lysosomal genes were generally unique to FTLD-TDP type A, regardless of *GRN* status.
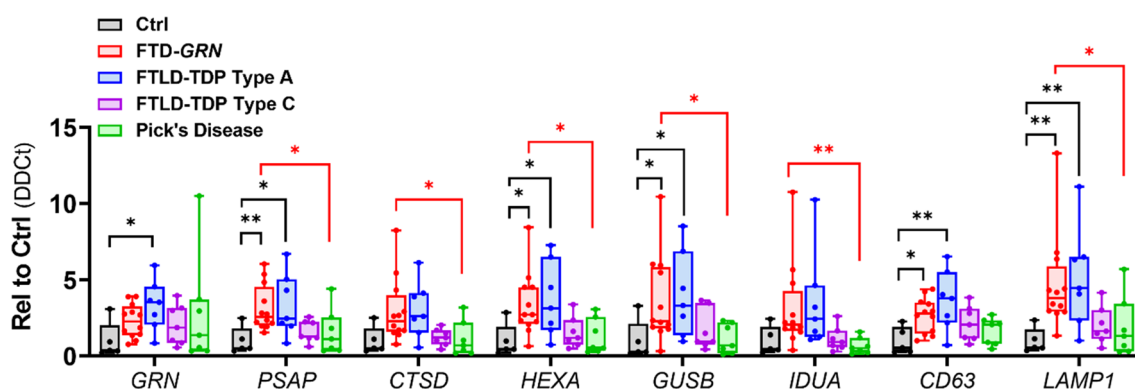

Fig. 6 Patients with Sporadic FTLD-TDP Type C or Pick's Disease Do Not Exhibit the Increased Lysosomal Gene Expression Observed in Patients with FTD-*GRN* or FTLD-TDP Type A. qPCR for a subset of lysosomal transcripts detected by Nanostring analysis (Fig. 2) generally validated their increased expression in frontal cortex of patients with FTD-*GRN* and sporadic FTLD-TDP type A (MANOVA effect of group, $p = 0.01$). However, none of these genes were significantly elevated from control in frontal cortex of patients with FTLD-TDP type C or Pick's disease. *$p < 0.05$, **$p < 0.01$ by Tukey's post-hoc test. Black lines and symbols indicate difference from control. Red lines and symbols indicate difference from FTD-*GRN*. n = 5 controls, 12 patients with FTD-*GRN*, 7 patients with FTLD-TDP type A, 7 patients with FTLD-TDP type C, and 7 patients with Pick's disease

Discussion

In this study, we report that many of the lysosomal abnormalities observed in frontal cortex of patients with FTD-*GRN* [8, 40, 90] are also present in frontal cortex of patients with several types of sporadic FTLD. Patients with sporadic FTLD-TDP types A and C and FTLD-tau (Pick's disease) exhibited similar increases in CatD activity, LAMP-1 and LAMP-2 levels, and lysosomal storage material as patients with FTD-*GRN*. Though we analyzed a limited number of FTLD subtypes, these data suggest that such lysosomal abnormalities may be a common feature of end-stage FTLD. These lysosomal abnormalities may be associated with multiple aspects of FTLD pathology and neurodegeneration.

The increases in neuronal CatD (Additional file 1: Fig. S1, Fig. 4) and lysosomal storage material (Additional file 1: Fig. S4) are consistent with prior studies of FTD-*GRN* [40, 90] and FTD-*CHMP2B* [28], and may be a sign of neuronal lysosomal dysfunction. Lysosomal dysfunction may be an important contributor to FTLD-TDP and FTLD-tau pathogenesis, as the endolysosomal and autophagy-lysosomal pathways clear TDP-43 and tau, and disruption of these pathways exacerbates both types of pathology [12, 53, 54, 78, 88, 89, 96]. Mutations in several genes involved in autophagy-lysosomal function cause FTLD-TDP [72, 86, 87], implicating lysosomal dysfunction in the initiation of FTLD-TDP. Additionally, both TDP-43 and tau pathology may disrupt lysosomal function, driving further pathology. Loss of nuclear TDP-43 is a key aspect of TDP-43 pathology [4, 65] that may disrupt the autophagy-lysosomal and endolysosomal systems [15, 71, 77, 95]. Pathologic tau can also inhibit autophagy [19, 20], and the FTD-causing R406W tau mutation disrupts lysosomal function in iPSC-derived neurons [60].

While lysosomal dysfunction is implicated in FTLD-TDP and FTLD-tau pathogenesis, the increased CatD and lysosomal storage material in FTLD might also be downstream of neurodegeneration. Similar increases in neuronal cathepsin D and lysosomal storage material have been observed in degenerated regions of brains from patients with Alzheimer's disease (AD) [21, 22], though these changes are closely associated with AD pathology [23]. Accumulation of lysosomal storage material has also been observed in models of stroke [9], excitotoxicity [48] and traumatic brain injury [45, 47, 70], perhaps indicating a general relationship with neuronal stress or death. In contrast, CatD levels increase in some models of injury and excitotoxicity [11, 13, 16], but decrease in models of hypoxia and stroke [61] and at early time points after traumatic brain injury [74].

Neuroinflammation may also drive some of the lysosomal abnormalities we observed in patients with sporadic FTLD. Degenerated brain regions in FTLD contain many reactive glia [52, 57], which strongly express lysosomal genes [75, 102, 103]. Reactive glia may drive several of the changes we observed, such as increased *GRN* expression in patients with FTD-*GRN* and sporadic FTLD-TDP A (Fig. 2, Additional file 1: S1) [25]. Glial phagocytosis of dead neurons may explain the presence of storage material in glial cells of patients with sporadic FTLD (Additional file 1: Fig. S7), as similar effects have been observed in microglia in rodent models of traumatic brain injury [45, 47, 70].

In summary, the increases in lysosomal proteins and storage material in patients with sporadic FTLD and FTD-*GRN* [8, 40, 90] may be driven by a combination of both dysfunctional neurons and reactive glia. Further investigation will be needed to determine if the increased CatD and storage material in neurons are an indicator of lysosomal dysfunction that may contribute to FTLD pathogenesis or a more non-specific indicator of neuronal distress and death.

This study also raises questions about the relationship between progranulin haploinsufficiency, lysosomal dysfunction, and FTLD-TDP pathology in patients with *GRN* mutations. Comparison of lysosomal measures in frontal and occipital cortices of patients with FTD-*GRN* and sporadic FTLD-TDP type A (Figs. 1, 2, 3, Additional file 1: S1, S2) suggests an association of lysosomal abnormalities with TDP-opathy, neurodegeneration, or inflammation rather than with progranulin haploinsufficiency. Notably, patients with FTD-*GRN* also exhibit lipofuscin accumulation, loss of nuclear TDP-43, and degeneration in the retina [90, 91]. These data may indicate that these lysosomal abnormalities are primarily driven by TDP-opathy, neurodegeneration, or neuroinflammation rather than by progranulin haploinsufficiency. If so, then progranulin haploinsufficiency, unlike complete progranulin deficiency, may produce relatively mild lysosomal dysfunction in the brain. This is also observed in mouse models. Brains from $Grn^{-/-}$ mice, which model the progranulin deficiency of NCL [2, 44, 82], exhibit robust lysosomal changes and lipofuscinosis [1, 31, 32, 40, 56, 83]. However, brains from $Grn^{+/-}$ mice, which model the progranulin haploinsufficiency of FTD-*GRN*, exhibit milder changes in lysosomal protein levels [5, 6, 31] and fail to accumulate lipofuscin [1, 32].

Alternatively, the association of lysosomal abnormalities with FTLD-TDP pathology in FTD-*GRN* may indicate regional differences in vulnerability to progranulin haploinsufficiency. Such vulnerability might arise via several mechanisms. In the retina, the daily cycle of photoreceptor degradation places high demand on lysosomes

in cells of the retinal pigment epithelium [51], which might make them more vulnerable to disruption by progranulin haploinsufficiency. Within the cortex, regional differences in progranulin cleavage might contribute to selective vulnerability. Greater progranulin cleavage into granulins might contribute to neurodegeneration, as progranulin and granulins have distinct effects on inflammation [108] and lysosomal protease activity [17, 18]. Mouse studies indicate differential cleavage of progranulin between brain regions, with the cortex having a particularly high granulin to progranulin ratio [101]. Patients with FTD-*GRN* exhibit greater cleavage of progranulin to granulins in a degenerated region of frontal cortex than in occipital cortex [63], but this higher cleavage of progranulin may be driven by neurodegeneration or inflammation, as it is also observed in degenerated regions of patients with sporadic FTLD-TDP type A and AD [73].

As in sporadic FTLD, the role of lysosomal dysfunction in FTD-*GRN* pathogenesis will therefore be an important topic for future investigation. The presence of similar lysosomal abnormalities in patients with FTD-*GRN*, patients with sporadic FTLD, and TDP++ mice shows that progranulin haploinsufficiency is not necessary to produce increases in some lysosomal proteins and storage material. However, this does not rule out progranulin haploinsufficiency as an early driver of lysosomal abnormalities in patients with FTD-*GRN*. For example, data from $Grn^{-/-}$ mice suggest a model in which progranulin deficiency induces lysosomal dysfunction in microglia [39, 56], which then drives neuronal dysfunction and TDP-opathy at later ages [39, 56, 100].

Despite similar signs of lysosomal dysfunction among all FTLD patient groups, patients with FTD-*GRN* and sporadic FTLD-TDP type A exhibited unique changes in expression of lysosomal genes (Figs. 2, 6). Patients with FTLD-TDP type A, regardless of *GRN* genotype, might therefore exhibit unique lysosomal changes compared to other FTLD subtypes. Patients with FTD-*GRN* or sporadic FTLD-TDP type A also exhibit unique transcriptional changes in other pathways, as a recent transcriptomic study showed substantial overlap in differentially-expressed genes among patients with FTD-*GRN* and sporadic FTLD-TDP type A, which diverged from changes in patients with FTLD-TDP type C [68]. Understanding the role of transcriptional dysregulation in FTLD-TDP type A pathogenesis is therefore another important area for future investigation.

Conclusions

This study shows that patients with several subtypes of sporadic FTLD have similar increases in CatD activity, lysosomal membrane proteins, and lysosomal storage

material as patients with FTD-*GRN*. These changes may be driven by lysosomal dysfunction associated with FTLD-TDP or FTLD-tau pathology, or with neurodegeneration and neuroinflammation. In contrast, the unique changes in lysosomal gene expression of patients with FTD-*GRN* and sporadic FTLD-TDP type A indicate lysosomal changes specific to FTLD-TDP type A. These data indicate that lysosomal abnormalities may be a common feature of end-stage FTLD, though they may be driven by distinct mechanisms in different FTLD subtypes.

Abbreviations

CatD	Cathepsin D
FTD	Frontotemporal dementia
FTD-*GRN*	Frontotemporal dementia due to progranulin mutations
FTLD	Frontotemporal lobar degeneration
GCase	β-Glucocerebrosidase
GRN	Progranulin
HexA	β-Hexosaminidase A
NCL	Neuronal ceroid lipofuscinosis
SCMAS	Subunit C of mitochondrial ATP synthase
TDP-43	TAR DNA binding protein of 43 kDa

Supplementary Information

The online version contains supplementary material available at https://doi.org/10.1186/s40478-023-01571-4.

> **Additional file 1: Fig. S1.** Quantitation of Low Molecular Weight GCase. **Fig. S2.** Correlation of Triton-insoluble 25 kDa p-TDP-43 with Levels of Lysosomal Proteins. **Fig. S3.** Progranulin, Cathepsin D, and GCase labeling by cell type. **Fig. S4.** Confirmation of TDP-43 aggregation in TDP-43 transgenic mice. **Fig. S5.** Further analysis of storage material in TDP-43 transgenic mice. **Fig. S6.** GCase Levels in Patients with Multiple FTLD Subtypes. **Fig. S7.** Cellular distribution of autofluorescent storage material in frontal cortex.
>
> **Additional file 2:** Tables of patient data.

Author contributions

AEA and WWS conceived the study and designed experiments. SED, AKC, JAH, YV, NVC, NRB, ARH, KMA, KPH, DAP, LJM, MS, KAM, and AEA performed the experiments. ALN, SS, LTG, BLM, and WWS characterized the patients, made neuropathological diagnoses, and provided brain samples. SED, CFM, RMC, and AEA analyzed the data. AEA wrote the initial manuscript and all authors provided comments and assisted with editing. All authors read and approved the final manuscript.

Davis *et al. Acta Neuropathologica Communications* (2023) 11:70

Page 16 of 19

Availability of data and materials

All data generated or analyzed during this study are included in this published article and supplemental material.

Declarations

Ethics approval and consent to participate

Brains were donated to the Neurodegenerative Disease Brain Bank at the University of California, San Francisco with the consent of the patients or their surrogates in accordance with the Declaration of Helsinki. The research was approved by the University of California, San Francisco Committee on Human Research. All animal experiments were approved by the Institutional Animal Care and Use Committee at the University of Alabama at Birmingham.

Consent for publication

Not applicable.

Competing interests

The authors declare that they have no competing interests.

Author details

[1]Department of Neurology, Center for Neurodegeneration and Experimental Therapeutics, Alzheimer's Disease Center, Evelyn F. McKnight Brain Institute, University of Alabama at Birmingham, Birmingham, AL, USA. [2]Department of Neurobiology, University of Alabama at Birmingham, Birmingham, AL, USA. [3]Department of Biostatistics, University of Alabama at Birmingham, Birmingham, AL, USA. [4]Department of Neuroscience, Southern Research, Birmingham, AL, USA. [5]Department of Neurology, Memory and Aging Center, UCSF Weill Institute for Neurosciences, University of California, San Francisco, San Francisco, CA, USA. [6]Department of Pathology, University of California, San Francisco, San Francisco, CA, USA.

References

1. Ahmed Z, Sheng H, Xu YF, Lin WL, Innes AE, Gass J, Yu X, Hou H, Chiba S, Yamanouchi K et al (2010) Accelerated lipofuscinosis and ubiquitination in granulin knockout mice suggest a role for progranulin in successful aging. Am J Pathol 177:311–324. https://doi.org/10.2353/ajpath.2010.090915
2. Almeida MR, Macario MC, Ramos L, Baldeiras I, Ribeiro MH, Santana I (2016) Portuguese family with the co-occurrence of frontotemporal lobar degeneration and neuronal ceroid lipofuscinosis phenotypes due to progranulin gene mutation. Neurobiol Aging 41(200):e201-205. https://doi.org/10.1016/j.neurobiolaging.2016.02.019
3. Amick J, Ferguson SM (2017) C9orf72: at the intersection of lysosome cell biology and neurodegenerative disease. Traffic 18:267–276. https://doi.org/10.1111/tra.12477
4. Arrant AE, Davis SE, Vollmer RM, Murchison CF, Mobley JA, Nana AL, Spina S, Grinberg LT, Karydas AM, Miller BL et al (2020) Elevated levels of extracellular vesicles in progranulin-deficient mice and FTD-GRN Patients. Ann Clin Transl Neurol. https://doi.org/10.1002/acn3.51242
5. Arrant AE, Filiano AJ, Unger DE, Young AH, Roberson ED (2017) Restoring neuronal progranulin reverses deficits in a mouse model of frontotemporal dementia. Brain 140:1447–1465. https://doi.org/10.1093/brain/awx060
6. Arrant AE, Nicholson AM, Zhou X, Rademakers R, Roberson ED (2018) Partial Tmem106b reduction does not correct abnormalities due to progranulin haploinsufficiency. Mol Neurodegener 13:32. https://doi.org/10.1186/s13024-018-0264-6
7. Arrant AE, Onyilo VC, Unger DE, Roberson ED (2018) Progranulin gene therapy improves lysosomal dysfunction and microglial pathology associated with frontotemporal dementia and neuronal ceroid lipofuscinosis. J Neurosci 38:2341. https://doi.org/10.1523/JNEUROSCI.3081-17.2018
8. Arrant AE, Roth JR, Boyle NR, Kashyap SN, Hoffmann MQ, Murchison CF, Ramos EM, Nana AL, Spina S, Grinberg LT et al (2019) Impaired beta-glucocerebrosidase activity and processing in frontotemporal dementia due to progranulin mutations. Acta Neuropathol Commun 7:218. https://doi.org/10.1186/s40478-019-0872-6
9. Baixauli-Martin J, Aliena-Valero A, Castello-Ruiz M, Burguete MC, Lopez-Morales MA, Munoz-Espin D, Torregrosa G, Salom JB (2022) Brain cell senescence: a new therapeutic target for the acute treatment of ischemic stroke. J Neuropathol Exp Neurol 81:614–620. https://doi.org/10.1093/jnen/nlac048
10. Baker M, Mackenzie IR, Pickering-Brown SM, Gass J, Rademakers R, Lindholm C, Snowden J, Adamson J, Sadovnick AD, Rollinson S et al (2006) Mutations in progranulin cause tau-negative frontotemporal dementia linked to chromosome 17. Nature 442:916–919
11. Banerjee M, Sasse VA, Wang Y, Maulik M, Kar S (2015) Increased levels and activity of cathepsins B and D in kainate-induced toxicity. Neuroscience 284:360–373. https://doi.org/10.1016/j.neuroscience.2014.10.003
12. Barmada SJ, Serio A, Arjun A, Bilican B, Daub A, Ando DM, Tsvetkov A, Pleiss M, Li X, Peisach D et al (2014) Autophagy induction enhances TDP43 turnover and survival in neuronal ALS models. Nat Chem Biol 10:677–685. https://doi.org/10.1038/nchembio.1563
13. Beel S, Moisse M, Damme M, De Muynck L, Robberecht W, Van Den Bosch L, Saftig P, Van Damme P (2017) Progranulin functions as a cathepsin D chaperone to stimulate axonal outgrowth in vivo. Hum Mol Genet. https://doi.org/10.1093/hmg/ddx162
14. Boland S, Swarup S, Ambaw YA, Malia PC, Richards RC, Fischer AW, Singh S, Aggarwal G, Spina S, Nana AL et al (2022) Deficiency of the frontotemporal dementia gene GRN results in gangliosidosis. Nat Commun 13:5924. https://doi.org/10.1038/s41467-022-33500-9
15. Bose JK, Huang CC, Shen CK (2011) Regulation of autophagy by neuropathological protein TDP-43. J Biol Chem 286:44441–44448. https://doi.org/10.1074/jbc.M111.237115
16. Braidy N, Brew BJ, Inestrosa NC, Chung R, Sachdev P, Guillemin GJ (2014) Changes in Cathepsin D and Beclin-1 mRNA and protein expression by the excitotoxin quinolinic acid in human astrocytes and neurons. Metab Brain Dis 29:873–883. https://doi.org/10.1007/s11011-014-9557-9
17. Butler VJ, Cortopassi WA, Argouarch AR, Ivry SL, Craik CS, Jacobson MP, Kao AW (2019) Progranulin stimulates the in vitro maturation of pro-cathepsin D at acidic pH. J Mol Biol 431:1038–1047. https://doi.org/10.1016/j.jmb.2019.01.027
18. Butler VJ, Cortopassi WA, Gururaj S, Wang AL, Pierce OM, Jacobson MP, Kao AW (2019) Multi-granulin domain peptides bind to pro-cathepsin D and stimulate its enzymatic activity more effectively than progranulin in vitro. Biochemistry 58:2670–2674. https://doi.org/10.1021/acs.biochem.9b00275
19. Caballero B, Bourdenx M, Luengo E, Diaz A, Sohn PD, Chen X, Wang C, Juste YR, Wegmann S, Patel B et al (2021) Acetylated tau inhibits chaperone-mediated autophagy and promotes tau pathology propagation in mice. Nat Commun 12:2238. https://doi.org/10.1038/s41467-021-22501-9
20. Caballero B, Wang Y, Diaz A, Tasset I, Juste YR, Stiller B, Mandelkow EM, Mandelkow E, Cuervo AM (2018) Interplay of pathogenic forms of human tau with different autophagic pathways. Aging Cell. https://doi.org/10.1111/acel.12692
21. Cataldo AM, Barnett JL, Berman SA, Li J, Quarless S, Bursztajn S, Lippa C, Nixon RA (1995) Gene expression and cellular content of cathepsin D in Alzheimer's disease brain: evidence for early up-regulation of the endosomal-lysosomal system. Neuron 14:671–680
22. Cataldo AM, Hamilton DJ, Nixon RA (1994) Lysosomal abnormalities in degenerating neurons link neuronal compromise to senile plaque

Davis *et al. Acta Neuropathologica Communications*   (2023) 11:70

Page 17 of 19

development in Alzheimer disease. Brain Res 640:68–80. https://doi.org/10.1016/0006-8993(94)91858-9

23. Cataldo AM, Thayer CY, Bird ED, Wheelock TR, Nixon RA (1990) Lysosomal proteinase antigens are prominently localized within senile plaques of Alzheimer's disease: evidence for a neuronal origin. BrainRes 513:181–192

24. Chang MC, Srinivasan K, Friedman BA, Suto E, Modrusan Z, Lee WP, Kaminker JS, Hansen DV, Sheng M (2017) Progranulin deficiency causes impairment of autophagy and TDP-43 accumulation. J Exp Med 214:2611–2628. https://doi.org/10.1084/jem.20160999

25. Chen-Plotkin AS, Xiao J, Geser F, Martinez-Lage M, Grossman M, Unger T, Wood EM, Van Deerlin VM, Trojanowski JQ, Lee VM (2010) Brain progranulin expression in GRN-associated frontotemporal lobar degeneration. Acta Neuropathol 119:111–122. https://doi.org/10.1007/s00401-009-0576-2

26. Chen Y, Jian J, Hettinghouse A, Zhao X, Setchell KDR, Sun Y, Liu CJ (2018) Progranulin associates with hexosaminidase A and ameliorates GM2 ganglioside accumulation and lysosomal storage in Tay-Sachs disease. J Mol Med 96:1359–1373. https://doi.org/10.1007/s00109-018-1703-0

27. Cirulli ET, Lasseigne BN, Petrovski S, Sapp PC, Dion PA, Leblond CS, Couthouis J, Lu YF, Wang Q, Krueger BJ et al (2015) Exome sequencing in amyotrophic lateral sclerosis identifies risk genes and pathways. Science 347:1436–1441. https://doi.org/10.1126/science.aaa3650

28. Clayton EL, Mizielinska S, Edgar JR, Nielsen TT, Marshall S, Norona FE, Robbins M, Damirji H, Holm IE, Johannsen P et al (2015) Frontotemporal dementia caused by CHMP2B mutation is characterised by neuronal lysosomal storage pathology. Acta Neuropathol 130:511–523. https://doi.org/10.1007/s00401-015-1475-3

29. Cruts M, Gijselinck I, van der Zee J, Engelborghs S, Wils H, Pirici D, Rademakers R, Vandenberghe R, Dermaut B, Martin JJ et al (2006) Null mutations in progranulin cause ubiquitin-positive frontotemporal dementia linked to chromosome 17q21. Nature 442:920–924

30. Elleder M, Sokolová J, Hřebíček M (1997) Follow-up study of subunit c of mitochondrial ATP synthase (SCMAS) in Batten disease and in unrelated lysosomal disorders. Acta Neuropathol 93:379–390. https://doi.org/10.1007/s004010050629

31. Evers BM, Rodriguez-Navas C, Tesla RJ, Prange-Kiel J, Wasser CR, Yoo KS, McDonald J, Cenik B, Ravenscroft TA, Plattner F et al (2017) Lipidomic and transcriptomic basis of lysosomal dysfunction in progranulin deficiency. Cell Rep 20:2565–2574. https://doi.org/10.1016/j.celrep.2017.08.056

32. Filiano AJ, Martens LH, Young AH, Warmus BA, Zhou P, Diaz-Ramirez G, Jiao J, Zhang Z, Huang EJ, Gao FB et al (2013) Dissociation of frontotemporal dementia–related deficits and neuroinflammation in progranulin haploinsufficient mice. J Neurosci 33:5352–5361. https://doi.org/10.1523/JNEUROSCI.6103-11.2013

33. Finch N, Baker M, Crook R, Swanson K, Kuntz K, Surtees R, Bisceglio G, Rovelet-Lecrux A, Boeve B, Petersen RC et al (2009) Plasma progranulin levels predict progranulin mutation status in frontotemporal dementia patients and asymptomatic family members. Brain 132:583–591. https://doi.org/10.1093/brain/awn352

34. Fox SN, McMeekin LJ, Savage CH, Joyce KL, Boas SM, Simmons MS, Farmer CB, Ryan J, Pereboeva L, Becker K et al (2022) Estrogen-related receptor gamma regulates mitochondrial and synaptic genes and modulates vulnerability to synucleinopathy. NPJ Parkinsons Dis 8:106. https://doi.org/10.1038/s41531-022-00369-w

35. Freischmidt A, Wieland T, Richter B, Ruf W, Schaeffer V, Muller K, Marroquin N, Nordin F, Hubers A, Weydt P et al (2015) Haploinsufficiency of TBK1 causes familial ALS and fronto-temporal dementia. Nat Neurosci 18:631–636. https://doi.org/10.1038/nn.4000

36. Ghidoni R, Benussi L, Glionna M, Franzoni M, Binetti G (2008) Low plasma progranulin levels predict progranulin mutations in frontotemporal lobar degeneration. Neurology 71:1235–1239. https://doi.org/10.1212/01.wnl.0000325058.10218.fc

37. Gijselinck I, Van Mossevelde S, van der Zee J, Sieben A, Philtjens S, Heeman B, Engelborghs S, Vandenbulcke M, De Baets G, Baumer V et al (2015) Loss of TBK1 is a frequent cause of frontotemporal dementia in a Belgian cohort. Neurology 85:2116–2125. https://doi.org/10.1212/WNL.0000000000002220

38. Gorno-Tempini ML, Hillis AE, Weintraub S, Kertesz A, Mendez M, Cappa SF, Ogar JM, Rohrer JD, Black S, Boeve BF et al (2011) Classification of primary progressive aphasia and its variants. Neurology 76:1006–1014. https://doi.org/10.1212/WNL.0b013e31821103e6

39. Gotzl JK, Colombo AV, Fellerer K, Reifschneider A, Werner G, Tahirovic S, Haass C, Capell A (2018) Early lysosomal maturation deficits in microglia triggers enhanced lysosomal activity in other brain cells of progranulin knockout mice. Mol Neurodegener 13:48. https://doi.org/10.1186/s13024-018-0281-5

40. Götzl JK, Mori K, Damme M, Fellerer K, Tahirovic S, Kleinberger G, Janssens J, van der Zee J, Lang CM, Kremmer E et al (2014) Common pathobiochemical hallmarks of progranulin-associated frontotemporal lobar degeneration and neuronal ceroid lipofuscinosis. Acta Neuropathol 127:845–860. https://doi.org/10.1007/s00401-014-1262-6

41. Hall NA, Lake BD, Dewji NN, Patrick AD (1991) Lysosomal storage of subunit c of mitochondrial ATP synthase in Batten's disease (ceroid-lipofuscinosis). Biochem J 275(Pt 1):269–272

42. Hashimoto K, Jahan N, Miller ZA, Huang EJ (2022) Neuroimmune dysfunction in frontotemporal dementia: insights from progranulin and C9orf72 deficiency. Curr Opin Neurobiol 76:102599. https://doi.org/10.1016/j.conb.2022.102599

43. Hu F, Padukkavidana T, Vægter CB, Brady OA, Zheng Y, Mackenzie IR, Feldman HH, Nykjaer A, Strittmatter SM (2010) Sortilin-mediated endocytosis determines levels of the frontotemporal dementia protein, progranulin. Neuron 68:654–667. https://doi.org/10.1016/j.neuron.2010.09.034

44. Huin V, Barbier M, Bottani A, Lobrinus JA, Clot F, Lamari F, Chat L, Rucheton B, Fluchere F, Auvin S et al (2019) Homozygous GRN mutations: new phenotypes and new insights into pathological and molecular mechanisms. Brain. https://doi.org/10.1093/brain/awz377

45. Jacobowitz DM, Cole JT, McDaniel DP, Pollard HB, Watson WD (2012) Microglia activation along the corticospinal tract following traumatic brain injury in the rat: a neuroanatomical study. Brain Res 1465:80–89. https://doi.org/10.1016/j.brainres.2012.05.008

46. Jian J, Tian QY, Hettinghouse A, Zhao S, Liu H, Wei J, Grunig G, Zhang W, Setchell KD, Sun Y et al (2016) Progranulin recruits HSP70 to beta-glucocerebrosidase and is therapeutic against gaucher disease. EBioMedicine 13:212–224. https://doi.org/10.1016/j.ebiom.2016.10.010

47. Kelley BJ, Lifshitz J, Povlishock JT (2007) Neuroinflammatory responses after experimental diffuse traumatic brain injury. J Neuropathol Exp Neurol 66:989–1001. https://doi.org/10.1097/NEN.0b013e3181588245

48. Kim HC, Bing G, Jhoo WK, Kim WK, Shin EJ, Park ES, Choi YS, Lee DW, Shin CY, Ryu JR et al (2002) Oxidative damage causes formation of lipofuscin-like substances in the hippocampus of the senescence-accelerated mouse after kainate treatment. Behav Brain Res 131:211–220. https://doi.org/10.1016/s0166-4328(01)00382-5

49. Klionsky DJ, Abdel-Aziz AK, Abdelfatah S, Abdellatif M, Abdoli A, Abel S, Abeliovich H, Abildgaard MH, Abudu YP, Acevedo-Arozena A et al (2021) Guidelines for the use and interpretation of assays for monitoring autophagy (4th edition)(1). Autophagy 17:1–382. https://doi.org/10.1080/15548627.2020.1797280

50. Kominami E, Ezaki J, Muno D, Ishido K, Ueno T, Wolfe LS (1992) Specific storage of subunit c of mitochondrial ATP synthase in lysosomes of neuronal ceroid lipofuscinosis (Batten's disease). J Biochem 111:278–282

51. Lakkaraju A, Umapathy A, Tan LX, Daniele L, Philp NJ, Boesze-Battaglia K, Williams DS (2020) The cell biology of the retinal pigment epithelium. Prog Retin Eye Res. https://doi.org/10.1016/j.preteyeres.2020.100846

52. Lant SB, Robinson AC, Thompson JC, Rollinson S, Pickering-Brown S, Snowden JS, Davidson YS, Gerhard A, Mann DM (2014) Patterns of microglial cell activation in frontotemporal lobar degeneration. Neuropathol Appl Neurobiol 40:686–696. https://doi.org/10.1111/nan.12092

53. Lee MJ, Lee JH, Rubinsztein DC (2013) Tau degradation: the ubiquitin-proteasome system versus the autophagy-lysosome system. Prog Neurobiol 105:49–59. https://doi.org/10.1016/j.pneurobio.2013.03.001

54. Liu G, Coyne AN, Pei F, Vaughan S, Chaung M, Zarnescu DC, Buchan JR (2017) Endocytosis regulates TDP-43 toxicity and turnover. Nat Commun 8:2092. https://doi.org/10.1038/s41467-017-02017-x

55. Logan T, Simon MJ, Rana A, Cherf GM, Srivastava A, Davis SS, Low RLY, Chiu CL, Fang M, Huang F et al (2021) Rescue of a lysosomal storage disorder caused by GRN loss of function with a brain penetrant progranulin biologic. Cell. https://doi.org/10.1016/j.cell.2021.08.002

Davis *et al. Acta Neuropathologica Communications*   (2023) 11:70

Page 18 of 19

56. Lui H, Zhang J, Makinson SR, Cahill MK, Kelley KW, Huang HY, Shang Y, Oldham MC, Martens LH, Gao F et al (2016) Progranulin deficiency promotes circuit-specific synaptic pruning by microglia via complement activation. Cell 165:921–935. https://doi.org/10.1016/j.cell.2016.04.001

57. Mackenzie IR, Baker M, Pickering-Brown S, Hsiung GY, Lindholm C, Dwosh E, Gass J, Cannon A, Rademakers R, Hutton M et al (2006) The neuropathology of frontotemporal lobar degeneration caused by mutations in the progranulin gene. Brain 129:3081–3090. https://doi.org/10.1093/brain/awl271

58. Mackenzie IR, Neumann M, Baborie A, Sampathu DM, Du Plessis D, Jaros E, Perry RH, Trojanowski JQ, Mann DM, Lee VM (2011) A harmonized classification system for FTLD-TDP pathology. Acta Neuropathol 122:111–113. https://doi.org/10.1007/s00401-011-0845-8

59. Mackenzie IR, Neumann M, Bigio EH, Cairns NJ, Alafuzoff I, Kril J, Kovacs GG, Ghetti B, Halliday G, Holm IE et al (2010) Nomenclature and nosology for neuropathologic subtypes of frontotemporal lobar degeneration: an update. Acta Neuropathol 119:1–4. https://doi.org/10.1007/s00401-009-0612-2

60. Mahali S, Martinez R, King M, Verbeck A, Harari O, Benitez BA, Horie K, Sato C, Temple S, Karch CM (2022) Defective proteostasis in induced pluripotent stem cell models of frontotemporal lobar degeneration. Transl Psychiatry 12:508. https://doi.org/10.1038/s41398-022-02274-5

61. Marcus JM, Hossain MI, Gagne JP, Poirier GG, McMahon LL, Cowell RM, Andrabi SA (2021) PARP-1 activation leads to cytosolic accumulation of TDP-43 in neurons. Neurochem Int 148:105077. https://doi.org/10.1016/j.neuint.2021.105077

62. Meeter LH, Patzke H, Loewen G, Dopper EG, Pijnenburg YA, van Minkelen R, van Swieten JC (2016) Progranulin levels in plasma and cerebrospinal fluid in granulin mutation carriers. Dement Geriatr Cogn Dis Extra 6:330–340. https://doi.org/10.1159/000447738

63. Mohan S, Sampognaro PJ, Argouarch AR, Maynard JC, Welch M, Patwardhan A, Courtney EC, Zhang J, Mason A, Li KH et al (2021) Processing of progranulin into granulins involves multiple lysosomal proteases and is affected in frontotemporal lobar degeneration. Mol Neurodegener 16:51. https://doi.org/10.1186/s13024-021-00472-1

64. Neary D, Snowden JS, Gustafson L, Passant U, Stuss D, Black S, Freedman M, Kertesz A, Robert PH, Albert M et al (1998) Frontotemporal lobar degeneration: a consensus on clinical diagnostic criteria. Neurology 51:1546–1554

65. Neumann M, Sampathu DM, Kwong LK, Truax AC, Micsenyi MC, Chou TT, Bruce J, Schuck T, Grossman M, Clark CM et al (2006) Ubiquitinated TDP-43 in frontotemporal lobar degeneration and amyotrophic lateral sclerosis. Science 314:130–133

66. Palop JJ, Mucke L, Roberson ED (2011) Quantifying biomarkers of cognitive dysfunction and neuronal network hyperexcitability in mouse models of Alzheimer's disease: depletion of calcium-dependent proteins and inhibitory hippocampal remodeling. Methods Mol Biol 670:245–262

67. Pottier C, Bieniek KF, Finch N, van de Vorst M, Baker M, Perkersen R, Brown P, Ravenscroft T, van Blitterswijk M, Nicholson AM et al (2015) Whole-genome sequencing reveals important role for TBK1 and OPTN mutations in frontotemporal lobar degeneration without motor neuron disease. Acta Neuropathol 130:77–92. https://doi.org/10.1007/s00401-015-1436-x

68. Pottier C, Mateiu L, Baker MC, DeJesus-Hernandez M, Teixeira Vicente C, Finch NA, Tian S, van Blitterswijk M, Murray ME, Ren Y et al (2022) Shared brain transcriptomic signature in TDP-43 type A FTLD patients with or without GRN mutations. Brain 145:2472–2485. https://doi.org/10.1093/brain/awab437

69. Rascovsky K, Hodges JR, Knopman D, Mendez MF, Kramer JH, Neuhaus J, van Swieten JC, Seelaar H, Dopper EG, Onyike CU et al (2011) Sensitivity of revised diagnostic criteria for the behavioural variant of frontotemporal dementia. Brain 134:2456–2477. https://doi.org/10.1093/brain/awr179

70. Ritzel RM, Doran SJ, Glaser EP, Meadows VE, Faden AI, Stoica BA, Loane DJ (2019) Old age increases microglial senescence, exacerbates secondary neuroinflammation, and worsens neurological outcomes after acute traumatic brain injury in mice. Neurobiol Aging 77:194–206. https://doi.org/10.1016/j.neurobiolaging.2019.02.010

71. Roczniak-Ferguson A, Ferguson SM (2019) Pleiotropic requirements for human TDP-43 in the regulation of cell and organelle homeostasis. Life Sci Alliance. https://doi.org/10.26508/lsa.201900358

72. Root J, Merino P, Nuckols A, Johnson M, Kukar T (2021) Lysosome dysfunction as a cause of neurodegenerative diseases: lessons from frontotemporal dementia and amyotrophic lateral sclerosis. Neurobiol Dis 154:105360. https://doi.org/10.1016/j.nbd.2021.105360

73. Salazar DA, Butler VJ, Argouarch AR, Hsu T-Y, Mason A, Nakamura A, McCurdy H, Cox D, Ng R, Pan G et al (2015) The progranulin cleavage products, granulins, exacerbate TDP-43 toxicity and increase TDP-43 levels. J Neurosci 35:9315–9328. https://doi.org/10.1523/JNEUROSCI.4808-14.2015

74. Sarkar C, Zhao Z, Aungst S, Sabirzhanov B, Faden AI, Lipinski MM (2014) Impaired autophagy flux is associated with neuronal cell death after traumatic brain injury. Autophagy 10:2208–2222. https://doi.org/10.4161/15548627.2014.981787

75. Saunders A, Macosko EZ, Wysoker A, Goldman M, Krienen FM, de Rivera H, Bien E, Baum M, Bortolin L, Wang S et al (2018) Molecular diversity and specializations among the cells of the adult mouse brain. Cell 174:1015-1030.e16. https://doi.org/10.1016/j.cell.2018.07.028

76. Schindelin J, Rueden CT, Hiner MC, Eliceiri KW (2015) The ImageJ ecosystem: an open platform for biomedical image analysis. Mol Reprod Dev 82:518–529. https://doi.org/10.1002/mrd.22489

77. Schwenk BM, Hartmann H, Serdaroglu A, Schludi MH, Hornburg D, Meissner F, Orozco D, Colombo A, Tahirovic S, Michaelsen M et al (2016) TDP-43 loss of function inhibits endosomal trafficking and alters trophic signaling in neurons. EMBO J 35:2350–2370. https://doi.org/10.15252/embj.201694221

78. Scotter EL, Vance C, Nishimura AL, Lee YB, Chen HJ, Urwin H, Sardone V, Mitchell JC, Rogelj B, Rubinsztein DC et al (2014) Differential roles of the ubiquitin proteasome system and autophagy in the clearance of soluble and aggregated TDP-43 species. J Cell Sci 127:1263–1278. https://doi.org/10.1242/jcs.140087

79. Sellami L, Rucheton B, Ben Younes I, Camuzat A, Saracino D, Rinaldi D, Epelbaum S, Azuar C, Levy R, Auriacombe S et al (2020) Plasma progranulin levels for frontotemporal dementia in clinical practice: a 10-year French experience. Neurobiol Aging 91:167.e1-167.e9. https://doi.org/10.1016/j.neurobiolaging.2020.02.014

80. Shiers S, Klein RM, Price TJ (2020) Quantitative differences in neuronal subpopulations between mouse and human dorsal root ganglia demonstrated with RNAscope in situ hybridization. Pain 161:2410–2424. https://doi.org/10.1097/j.pain.0000000000001973

81. Skibinski G, Parkinson NJ, Brown JM, Chakrabarti L, Lloyd SL, Hummerich H, Nielsen JE, Hodges JR, Spillantini MG, Thusgaard T et al (2005) Mutations in the endosomal ESCRTIII-complex subunit CHMP2B in frontotemporal dementia. Nat Genet 37:806–808

82. Smith KR, Damiano J, Franceschetti S, Carpenter S, Canafoglia L, Morbin M, Rossi G, Pareyson D, Mole SE, Staropoli JF et al (2012) Strikingly different clinicopathological phenotypes determined by progranulin-mutation dosage. Am J Hum Genet 90:1102–1107. https://doi.org/10.1016/j.ajhg.2012.04.021

83. Tanaka Y, Chambers JK, Matsuwaki T, Yamanouchi K, Nishihara M (2014) Possible involvement of lysosomal dysfunction in pathological changes of the brain in aged progranulin-deficient mice. Acta Neuropathol Commun 2:78. https://doi.org/10.1186/s40478-014-0078-x

84. Valdez C, Wong YC, Schwake M, Bu G, Wszolek ZK, Krainc D (2017) Progranulin-mediated deficiency of cathepsin D results in FTD and NCL-like phenotypes in neurons derived from FTD patients. Hum Mol Genet. https://doi.org/10.1093/hmg/ddx364

85. Valdez C, Ysselstein D, Young TJ, Zheng J, Krainc D (2020) Progranulin mutations result in impaired processing of prosaposin and reduced glucocerebrosidase activity. Hum Mol Genet 29:716–726. https://doi.org/10.1093/hmg/ddz229

86. Wallings RL, Humble SW, Ward ME, Wade-Martins R (2019) Lysosomal dysfunction at the Centre of Parkinson's disease and frontotemporal dementia/amyotrophic lateral sclerosis. Trends Neurosci 42:899–912. https://doi.org/10.1016/j.tins.2019.10.002

87. Wang C, Telpoukhovskaia MA, Bahr BA, Chen X, Gan L (2018) Endolysosomal dysfunction: a converging mechanism in neurodegenerative diseases. Curr Opin Neurobiol 48:52–58. https://doi.org/10.1016/j.conb.2017.09.005

88. Wang IF, Guo BS, Liu YC, Wu CC, Yang CH, Tsai KJ, Shen CK (2012) Autophagy activators rescue and alleviate pathogenesis of a mouse model with proteinopathies of the TAR DNA-binding protein 43. Proc Natl Acad Sci USA 109:15024–15029. https://doi.org/10.1073/pnas.1206362109

89. Wang Y, Martinez-Vicente M, Kruger U, Kaushik S, Wong E, Mandelkow EM, Cuervo AM, Mandelkow E (2009) Tau fragmentation, aggregation and clearance: the dual role of lysosomal processing. Hum Mol Genet 18:4153–4170. https://doi.org/10.1093/hmg/ddp367

90. Ward ME, Chen R, Huang HY, Ludwig C, Telpoukhovskaia M, Taubes A, Boudin H, Minami SS, Reichert M, Albrecht P et al (2017) Individuals with progranulin haploinsufficiency exhibit features of neuronal ceroid lipofuscinosis. Sci Transl Med. https://doi.org/10.1126/scitranslmed.aah5642

91. Ward ME, Taubes A, Chen R, Miller BL, Sephton CF, Gelfand JM, Minami S, Boscardin J, Martens LH, Seeley WW et al (2014) Early retinal neuro-degeneration and impaired Ran-mediated nuclear import of TDP-43 in progranulin-deficient FTLD. J Exp Med 211:1937–1945. https://doi.org/10.1084/jem.20140214

92. Watts GD, Wymer J, Kovach MJ, Mehta SG, Mumm S, Darvish D, Pestronk A, Whyte MP, Kimonis VE (2004) Inclusion body myopathy associated with Paget disease of bone and frontotemporal dementia is caused by mutant valosin-containing protein. Nat Genet 36:377–381

93. Wils H, Kleinberger G, Janssens J, Pereson S, Joris G, Cuijt I, Smits V, Ceuterick-de Groote C, Van Broeckhoven C, Kumar-Singh S (2010) TDP-43 transgenic mice develop spastic paralysis and neuronal inclusions characteristic of ALS and frontotemporal lobar degeneration. Proc Natl Acad Sci USA 107:3858–3863. https://doi.org/10.1073/pnas.0912417107

94. Wu Y, Shao W, Todd TW, Tong J, Yue M, Koga S, Castanedes-Casey M, Librero AL, Lee CW, Mackenzie IR et al (2021) Microglial lysosome dysfunction contributes to white matter pathology and TDP-43 pro-teinopathy in GRN-associated FTD. Cell Rep 36:109581. https://doi.org/10.1016/j.celrep.2021.109581

95. Xia Q, Wang H, Hao Z, Fu C, Hu Q, Gao F, Ren H, Chen D, Han J, Ying Z et al (2016) TDP-43 loss of function increases TFEB activity and blocks autophagosome-lysosome fusion. EMBO J 35:121–142. https://doi.org/10.15252/embj.201591998

96. Xu Y, Propson NE, Du S, Xiong W, Zheng H (2021) Autophagy deficiency modulates microglial lipid homeostasis and aggravates tau pathology and spreading. Proc Natl Acad Sci USA. https://doi.org/10.1073/pnas.2023418118

97. Yasuda Y, Kageyama T, Akamine A, Shibata M, Kominami E, Uchiyama Y, Yamamoto K (1999) Characterization of new fluorogenic substrates for the rapid and sensitive assay of cathepsin E and cathepsin D. J Biochem 125:1137–1143

98. Yen JC, Chang FJ, Chang S (1995) A new criterion for automatic multi-level thresholding. IEEE Trans Image Process 4:370–378. https://doi.org/10.1109/83.366472

99. Zack GW, Rogers WE, Latt SA (1977) Automatic measurement of sister chromatid exchange frequency. J Histochem Cytochem 25:741–753. https://doi.org/10.1177/25.7.70454

100. Zhang J, Velmeshev D, Hashimoto K, Huang YH, Hofmann JW, Shi X, Chen J, Leidal AM, Dishart JG, Cahill MK et al (2020) Neurotoxic micro-glia promote TDP-43 proteinopathy in progranulin deficiency. Nature. https://doi.org/10.1038/s41586-020-2709-7

101. Zhang T, Du H, Santos MN, Wu X, Pagan MD, Trigiani LJ, Nishimura N, Reinheckel T, Hu F (2022) Differential regulation of progranulin derived granulin peptides. Mol Neurodegener 17:15. https://doi.org/10.1186/s13024-021-00513-9

102. Zhang Y, Chen K, Sloan SA, Bennett ML, Scholze AR, O'Keeffe S, Phatnani HP, Guarnieri P, Caneda C, Ruderisch N et al (2014) An RNA-sequencing transcriptome and splicing database of glia, neurons, and vascular cells of the cerebral cortex. J Neurosci 34:11929–11947. https://doi.org/10.1523/JNEUROSCI.1860-14.2014

103. Zhang Y, Sloan SA, Clarke LE, Caneda C, Plaza CA, Blumenthal PD, Vogel H, Steinberg GK, Edwards MS, Li G et al (2016) Purification and charac-terization of progenitor and mature human astrocytes reveals transcrip-tional and functional differences with mouse. Neuron 89:37–53. https://doi.org/10.1016/j.neuron.2015.11.013

104. Zhou X, Paushter DH, Feng T, Pardon CM, Mendoza CS, Hu F (2017) Regulation of cathepsin D activity by the FTLD protein progranulin. Acta Neuropathol. https://doi.org/10.1007/s00401-017-1719-5

105. Zhou X, Paushter DH, Pagan MD, Kim D, Nunez Santos M, Lieberman RL, Overkleeft HS, Sun Y, Smolka MB, Hu F (2019) Progranulin deficiency leads to reduced glucocerebrosidase activity. PLoS ONE 14:e0212382. https://doi.org/10.1371/journal.pone.0212382

106. Zhou X, Sun L, Bastos de Oliveira F, Qi X, Brown WJ, Smolka MB, Sun Y, Hu F (2015) Prosaposin facilitates sortilin-independent lysosomal traf-ficking of progranulin. J Cell Biol 210:991–1002. https://doi.org/10.1083/jcb.201502029

107. Zhou X, Sun L, Bracko O, Choi JW, Jia Y, Nana AL, Brady OA, Hernan-dez JCC, Nishimura N, Seeley WW et al (2017) Impaired prosaposin lysosomal trafficking in frontotemporal lobar degeneration due to progranulin mutations. Nat Commun 8:15277. https://doi.org/10.1038/ncomms15277

108. Zhu J, Nathan C, Jin W, Sim D, Ashcroft GS, Wahl SM, Lacomis L, Erdjument-Bromage H, Tempst P, Wright CD et al (2002) Conversion of proepithelin to epithelins: roles of SLPI and elastase in host defense and wound repair. Cell 111:867–878

Publisher's Note